Polish J. Chem., **78**, 463–514 (2004) **REVIEW ARTICLE**

Hydride[1] Formation, Magnetic and Transport Properties of Nickel and Nickel-Based Alloys

by H.J. Bauer[a] and F.E. Wagner[b]

[a]*Sektion Physik, Ludwig-Maximilians-Universität, D-80799 München, Germany*
[b]*Physik-Department E15, Technische Universität München, D-85747 Garching, Germany*

(Received December 5th, 2003)

Dedicated to Prof. Dr. B. Baranowski in honour of his pioneering work on the nickel-hydrogen system and on the occasion of the 45th anniversary of the discovery of nickel hydride.

We review the discovery of hydride formation in nickel and discuss how the incorporation of interstitial hydrogen into the metal lattice of nickel and some nickel-based alloys affects the magnetic and transport properties.

Key words: nickel, nickel-based alloys, hydrides, magnetism, electrical conductivity, high pressure

CONTENTS

---

[1] for both isotopes.

Many metals form hydrides by incorporating hydrogen on interstitial sites. Such systems have been the subject of extended studies, and their synthesis and understanding is still a challenge for both experimentalists and theorists. General reviews on these subjects have been given by various authors [1–5]. In this review we will focus on the hydrides of nickel and nickel-based alloys. The incorporation of hydrogen into d-transition metals affects the filling of the d-band and, as a consequence, the density of states at the Fermi level. This leads to remarkable changes of physical properties, such as the electrical conductivity, the specific heat, and last but not least, the magnetic behaviour.

Nickel hydride was first reported in 1959 by Baranowski and Smialowski [6] who, by continuing preceding promising experiments [7], succeeded in hydrogenating nickel electrolytically by lacing the electrolyte with promotors, and whose theory proved to the most successful. This was nearly a century after palladium, the 4d homologue of nickel, was found to take up hydrogen, when used as cathode in an electrolytic cell [8,9]. The hydride of nickel was the first hydride of a ferromagnetic metal of the iron group ever obtained. As palladium looses its strong Pauli type paramagnetism, when it is hydrogenated [10], nickel looses its ferromagnetism by hydrogenation [11–13]. In either case, the influence on the magnetic properties of the metal can be understood as a consequence of the filling of the d-band of the transition metal with electrons donated by the hydrogen. This conception was also supported by the disappearance of a step at the X-ray K-absorption edge of nickel on hydrogenation [14].

Like palladium hydride, nickel hydride is formed by an isomorphous transformation, in which the metal sublattice expands, but retains its fcc structure [15,16]. The hydrogen occupies the octahedral interstitial sites [17]. The complete filling of these sites corresponds to a hydrogen-to-metal ratio of $x = 1$ and a sodium chloride structure. Again, like in the case of palladium [9], there is a miscibility gap in the Ni-H system [6,11,13,18], which at ambient temperatures exists either as the α-phase, containing but very little hydrogen, or as the hydrogen-rich β-phase, for which compositions of $0.7 \leq x \leq 1.0$ at ambient temperature have been reported [6], but which appears to have H/metal ratios that are rather close to unity. Since the lattice parameter of nickel is about 10% smaller than that of palladium, the relative lattice expansion of 5.6% fully hydrogenated nickel is substantially larger than that of palladium with about 3.6% [9,15]. This may be one of the reasons, why it is more difficult to hydrogenate nickel than palladium, *i.e.* that in case of nickel a much higher hydrogen activity (about 8 orders of magnitude) on the surface is needed.

The formation of nickel hydride by contact of the metal with gaseous molecular hydrogen was initiated in the early sixties, when Baranowski tried to suppress the loss of hydrogen from electrolytically produced nickel hydride by compressing hydride pellets in a steel piston apparatus, producing there under self sealing quasi-hydrostatic pressures up to 2 GPa [19]. In subsequent experiments with a high pressure cell, that was specially designed to prevent hydrogen losses and in connection with a special kind of preparation for a now necessary large amount of nickel hydride [20], the decay of nickel hydride could indeed be halted merely by the hydrogen pressure built

up by the own hydrogen desorbed from the hydride [21,22]. In such experiments the decomposition pressure of nickel hydride could be determined to be 0.34 GPa at 25°C [21,22].

Due to hysteresis it was obvious that the formation of Ni-H_β required a higher hydrogen pressure. This was proved by adding nickel foils to the set of decomposing nickel hydride tablets; a formation of nickel hydride was never found [22]. Therefore, the development of a cylinder-piston device allowing the compression of hydrogen gas to a pressure of about 1 GPa was required. This finally resulted in the first synthesis of nickel hydride by direct contact of the metal with molecular hydrogen in the GPa range [23]. The high pressure synthesis of nickel hydride was in fact the first high pressure synthesis of a hydride. It stimulated the development of high pressure equipment suitable for *in situ* measurements of physical properties of such systems [24,25] and, moreover, opened the way for other high pressure techniques to obtain new metal hydrides (use of hydrides as hydrogen donor [26], of diamond anvil cell technique [27]).

1. Preliminary explanation of magnetic and electric properties with respect to the following sections

'Magnetization' measurements have turned out to be an extremely sensitive tool for studying the hydrogenation of nickel, since the loss of the spontaneous magnetization of nickel on hydrogenation can be detected much easier than, for instance, the suppression of the paramagnetism in the Pd-H system. Since α-NiH_x is ferromagnetic and β-NiH_x is not, the observation of the decrease and recovery of the spontaneous magnetization during hydrogenation or degassing can be used as a sensitive, *non-destructive* method of monitoring the α-β phase transition and studying the hydrogen absorption and desorption kinetics in nickel and many nickel-based alloys, both during electrolysis [11–13,28,29], section 3, and in high pressure cells [26,30,31], sections 2 and 6.

Further metal physical information can be obtained from the often considerable changes of the *temperature dependence* of the saturation magnetization, $M_S(T)$. This is particularly true of the 'Curie temperature'. For pure nickel the Curie temperature, $T_C = 358$°C, is rather high and high hydrogen pressures are needed to render the Curie region accessible to hydrogenation studies (section 5), but alloying with elements like copper lowers the Curie temperature sufficiently for the region of the Curie temperature to become accessible even to cathodic hydrogenation [32–34]. In the second half of the sixties the hydrogenation of alloys by promoter-assisted electrolysis was in fact studied in this way, including X-ray diffraction analysis [32–37]. These investigations, as well as studies of the hydrides of nickel-chromium alloys [38], yielded the first data on the properties of the hydrides of nickel alloys.

Magnetic *in situ* measurements of the *shape hysteresis loop* or of parameters like the 'coercitivity' or the 'remanence' often provide further insight into the processes taking place during the 'formation' of the hydride phase [13,28,29] and during the precipitation-like 'decomposition' of the hydride [11,13,28,29] (section 3).

'Mössbauer spectroscopy' has also turned out to be a valuable tool for studying the magnetic properties as well as the microscopic structure of nickel hydride, although it requires the introduction of a probe isotope into the nickel lattice, since the Mössbauer resonances in nickel itself are not well suited for routine studies. On the other hand, Mössbauer spectroscopy in this way maked it possible to study the diffusion and distribution of hydrogen-near impurities in the nickel lattice (section 4).

The ferromagnetism of nickel further allows the application of *metallographic decoration* techniques to depict details of the process of decomposition of the hydride phase [39]. Together with optical micrography, such experiments yielded convincing visual support for observations by other, less direct methods (section 5).

The high concentration of interstitial hydrogen in the metal matrix of the presented hydrides, connected with large lattice expansion as mentioned, leads to drastic metallurgical consequences, comparable to those occurring at common alloys. That suggests the application of conventional methods – here of the 'magnetothermal analysis' using significant changes of the temperature dependence of the saturation magnetization – for studying the constitution of metal hydrides as demonstrated on sequences of Ni-Cu and Ni-Cr alloys (section 5).

The above-mentioned possibility to obtain nickel-based hydrides by application of *high pressure gaseous hydrogen* opened new possibilities of intending the research among others especially in connection with suitable devices towards higher temperatures and so has helped to enlarge the knowledge about these systems (section 2 and 6).

The research concerning the influence of *hydrogen isotopy* on nickel-based metal-hydrogen systems was begun by Baranowski already in 1962 [40] and it rests upon the aforesaid methods. The hitherto existing results, also in analogy to palladium and alloys its, among other things show reversed kinetic isotope effects and suggest comparison with theoretical findings (section 7).

The 'electrical conductivity' is another property that can easily be studied *in situ* during cathodic and during high pressure charging with hydrogen. The behaviour of the electrical resistance on hydrogenation is generally dominated by the scattering of electrons on lattice sites with the interstitial hydrogen, leading to an increase of the residual resistance and on the other hand in case of magnetic materials to a decrease of the temperature dependence of the resistance, due to the decrease of the s-d-scattering, because of the neutralization of the magnetic moments by filling of the d-holes by the hydrogen electrons [41–43].

In case of nickel and its ferromagnetic alloys, the electron scattering is sensitive to the spontaneous magnetization and gives rise to the ferromagnetic resistance anomaly [44]. Already the first measurements of the electrical conductivity of $Ni_{0.7}Cu_{0.3}$ alloys during cathodic hydrogenation [32] drastically reflected the suppression of the ferromagnetic resistance anomaly in the region of the Curie temperature by the inter-

stitial hydrogen, and conversely demonstrated the ferromagnetic origin of this anomaly.

A separate direction of investigations – grouped in Section 8 – led to findings which *conversely* let the hydrogen also appear appropriate as a tool for analysing magnetic conditions, as *e.g.* gave rise to *anomalies* at nickel-based alloys, which are also expressed in *transport properties*, because of the neutralization of the matrix ferromagnetism in connection with the interstitial insertion of the hydrogen. The reason for these appearances – according to the alloy partner and its concentration – is to be seen in the separation of local magnetic moments of 'impurities' or in the isolation of 'giant moments' in connection with 'cluster' magnetism. The magnetic character of such phenomena can be tested directly by magnetic measurements, but more easily by measurements of the electrical resistance of such metal-hydrogen systems under the influence of magnetic fields, *i.e.* of the 'magnetoresistance'.

By means of selected examples the following sections may now show the effect of the incorporation of interstitial hydrogen, as well as of deuterium, into the metal matrix of nickel and nickel-based alloys on its magnetic and transport properties.

2. Phenomenological phase-surface of a metal-hydrogen system for placing experimental findings

For a comprehensive understanding of the complex correlations of pressure, temperature and the atomic ratio of H/Me of such metal-hydrogen systems under thermodynamic equilibrium conditions, a schematic conception for P-T-C 'phase diagrams' of the metal-hydrogen systems, mentioned before, will be helpful in order to place experimental findings.

Fig. 1 shows a qualitative three-dimensional phase-surface of a fictive metal-hydrogen system with a ferromagnetic starting-matrix [49]. The scheme figures present the different regions of hydrogen concentrations under thermodynamic equilibrium conditions and the possible magnetic state connected with them.

On the left the low-concentrated α-phase is placed, which – according to the position of the Curie temperature – corresponds to the ferromagnetic state concerning 'primary' ferromagnetic properties as saturation magnetization and Curie temperature under normal conditions, which is practically not influenced by hydrogen. Here, however, 'secondary' magnetic phenomena, like hydrogen-induced after-effects [50], can take place. The right part of Fig. 1 represents a high concentrated β-phase, being in many cases non-ferromagnetic.

Between these regions of pure α- and pure β-phase, below the 'critical point' of phase separation, α- and β-phases coexist and correspondingly the ferromagnetic and the non-ferromagnetic state, as could be found for the first time in 1961 by magnetic measurements 'in situ' during the electrochemical hydrogenation of nickel [11]. It turned out that the saturation magnetization of nickel decreases linearly with increasing hydrogen content up to an atomic hydrogen-to-nickel ratio H/Ni of about 0.7, where ferromagnetism disappears [11,13]. In analogy to the Pd-H system, the *lineari-*

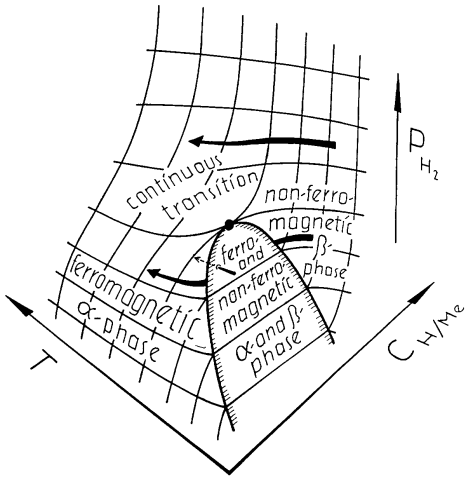

Figure 1. Assumed phase-surface of a metal-hydrogen system with a ferromagnetic α-phase and a ferro- or non-ferromagnetic β-phase.
• critical point of phase separation [49].

ty implies the existence of a large miscibility gap, *i.e.* the coexistence of two phases: the aforesaid ferromagnetic α-phase with H/Ni below about 0.03 and the non-ferromagnetic β-phase with H/Ni > 0.7. In this region the useful magnetic investigations on the kinetics of the mentioned hydride formation and decomposition processes become possible [29].

Above the critical point – in the one-phase region of solid solution – a continuous magnetic transition in dependence on the concentration of the hydrogen seems to occur.

Of course each alloy system has its own 'phase-surface', which moreover also depends on different metallurgical processes in the alloy matrix, that may occur in dependence on the hydrogenation conditions.

Generally, it is an essential goal to explore corresponding phase-surfaces under thermodynamic equilibrium conditions. In most of the presented alloys, however, these conditions can scarcely be defined quantitatively in an electrochemical way, but – as mentioned above – in all cases by the application of high pressure hydrogen [52,53]. This is valid in particular for the considered metal-hydrogen systems, whereby the useful evaluation of their ferromagnetic nature, including the Curie temperature (Ni: 631 K) for determining corresponding phase transitions – because of the instability of these systems, which sets in already under normal conditions – necessarily requires the application of a high pressure of gaseous hydrogen in GPa range. These demands are not easy to accomplish, because of the necessity to combine high pressure and high temperature techniques applied to gaseous hydrogen.

In this stage, in the middle of the 1970s, first experiments could be started concerning magnetic 'in situ' measurements at the system Ni-H_x under high hydrogen pressures: As an outcome of a cooperation of the University of Munich with B. Baranowski of the Polish Academy of Sciences in Warsaw, it became possible to record the change of the saturation magnetization of Ni-H_x during the hydride formation under high pressure gaseous hydrogen by a specially developed miniature magnetometer [30,31]. At the same time and independently, the high pressure group under E.G. Ponyatovsky of the Russian Academy of Science in Chernogolovka succeeded in recording the change of the Curie temperature of Ni during high pressure hydrogenation by applying a differential transformer method [26].

It should be mentioned here that the Russian group developed a special method for obtaining high hydrogen pressures. The method bases on avoiding an external hydrogen source and on using a hydride placed in the high-pressure chamber as a donor of hydrogen, due to decomposition by heating, and has so allowed to extend investigations under hydrogen pressures up to about 9 GPa at temperatures from about –150°C to 500°C. This possibility enabled the Russian scientists to synthesize further hydrides of transition metals of the groups VI to VIII in the periodic table as *e.g.* of iron, cobalt, molybdenum, rhodium, technetium, and the exploration of corresponding phase diagrams [42–46]. For an extended review see [43].

Hydrogen in this device was not pure, but included organic compounds – thus, the real hydrogen activity was surely lower than the one calculated from the pressure applied. This results in lower formation pressures of the hydrides in pure hydrogen environment.

In the following, within the scope of the outlined development of the nickel hydride research, we are dealing with some investigations of these systems performed in Munich and such carried out in cooperation with B. Baranowski in Warsaw, in the first place based on their magnetic behaviour.

3. Investigations at cathodical hydrogenation of nickel and nickel alloys. Formation and decomposition of the hydride phase

The interstitial hydrogen insertion in nickel, accompanied by the cancellation of its spontaneous magnetization, correspondingly also delivers successively lowered curves for the temperature dependence of its saturation magnetization, $M_s(T)$, which remain similar to the starting curve with no change of the Curie temperature T_C. That corresponds to the reduction of the magnetically effective cross section by a frontal progression of the non-ferromagnetic hydride phase in the sample (from both surfaces of a flat foil) and can be used for following the kinetics of the *hydrogen absorption* 'in situ' [28]: see *e.g.* Fig. 2. The proportionality already mentioned between the change in saturation magnetization and the change in the amount of interstitially absorbed hydrogen [11,13] can be expressed by

$$\frac{M_S}{M_{SO}} = 1 - \frac{m_t}{m_e} \tag{1}$$

where m_e is the final amount (*i.e.* M_S= O), and m_t the amount of hydrogen absorbed by nickel up to time *t*.

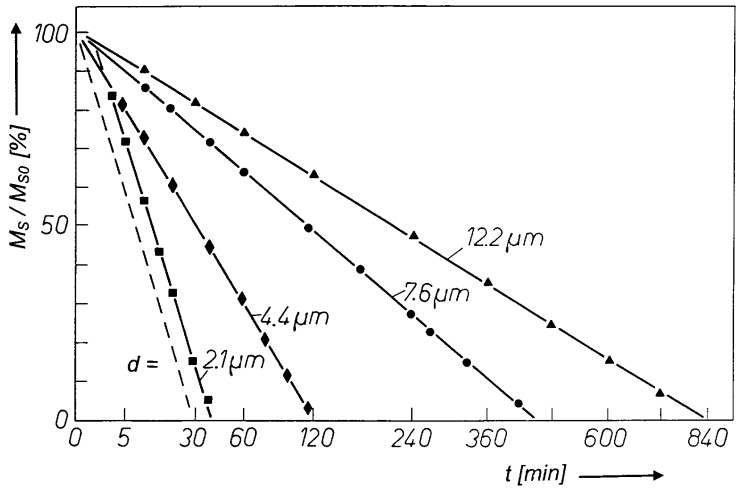

Figure 2. The linear decrease of the saturation magnetization M_S of nickel foils of different thicknesses during hydrogen charging (at 15.3°C), plotted against a quadratic time scale in connection with the foil thickness, confirms the $\sqrt{t}$ – law for diffusion. M_{SO} means the saturation magnetization of the uncharged samples [29].

The square root dependence at the absorption of hydrogen in nickel to be seen from Fig. 2 also results from the sequence of metallographic cross section pictures of Ni-foils, Fig. 3, which were exposed to cathodic hydrogenation for different times and, after 'outgassing' or desorption of the hydrogen and due to remaining visible crystal comminution, confirm the frontal diffusive character of the advancing hydride phase with direct measurable penetration depth [62,63].

In connection with the respective quantity of absorbed hydrogen a trapezoidal concentration profile can be confirmed, which is practically preserved until the fronts meet in the middle of the sample foil: Fig. 4 [29,62,63]. This is in accordance with the magnetic results.

The time dependence of the reduced saturation magnetization is well represented by

$$\frac{M_S}{M_{SO}} = 1 - \frac{1}{d}\sqrt{\frac{D}{2} \cdot \frac{c_0 - c_1}{c_1}}\sqrt{t} \tag{2}$$

where d is the thickness of the foil, D an average value of the diffusion coefficient for hydrogen in the β-phase, c_0 the hydrogen concentration at the surface of the foil, c_1 the concentration of hydrogen at the β/α interface, and t the charging time.

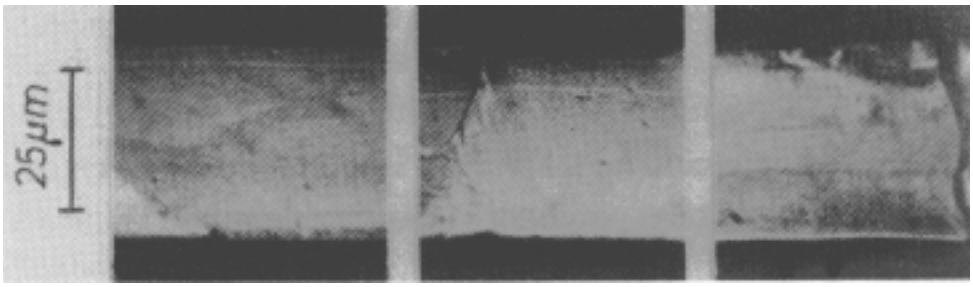

Figure 3. Optical micrographs of cross sections of Ni-foils after cathodic hydrogenation during 4^h, 16^h, 48^h (at 33.4°C), followed by desorption of the hydrogen, showing increasing penetration depths of the hydride phase by means of frontal crystallite cracks caused by the jump of lattice parameters (about 6% [15]) between β- and α-phase.

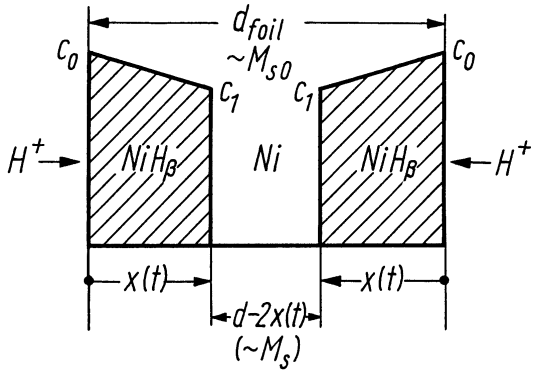

Figure 4. Scheme of the concentration profile (c_0, c_1) of the advancing hydride phase (NiH_β) in a nickel foil of the thickness d during cathodic charging with hydrogen [29]. $x(t)$ time-dependent penetration depth; M_S, M_{SO} as in Fig 2.

In agreement with corresponding measurements of the electrical resistance, also performed 'in situ' with an alternating-current bridge [64], the magnetic measurements for the interstitial insertion of the hydrogen in nickel yield a diffusion coefficient of about 10^{-10}–10^{-11} cm^2/s [29], *i.e.* some orders of magnitude lower in comparison with the case of palladium with around 10^{-7} cm^2/s [9].

Measuring methods of this direct kind in view of the metallurgical process also permit the determination of apparent activation energies E_a, which for the process of hydride formation in case of the Ni-H delivered the value $E_a \approx 27$ kJ/mol [29].

As to the *decomposition* of the nickel hydride in connection with the desorption of hydrogen, the magnetic determination delivers values up to 58 kJ/mol for the apparent activation energy E_a [29]. Compared to the process of hydride formation, in case

of decomposition of the hydride, the course of 'primary' and of 'secondary' ferromagnetic properties – characteristics of metallurgical processes in common alloys –, too, indicates a clear difference of mechanism. There have already been a few investigations dealing with this problem [11,28,65–67], which in addition to a change in the temperature dependence of the saturation magnetization M_S, show a change of the hysteresis loop *i.e.* of its characteristic quantities as of remanence I_r and especially of the coercivity H_c, which is passing a maximum in the time slope during the decomposition of nickel hydride.

These investigations have led to the conception that hydrogen during decomposition does not leave behind a more or less uniform region of pure nickel, but preferably starts at internal surfaces in the form of grain boundaries and lattice imperfections, which are distributed over the whole sample in a manner comparable to precipitation, whereby small ferromagnetic particles arise in a non-ferromagnetic matrix: we receive a picture known *e.g.* at heat treatment of the common nickel-copper alloys with small iron contents, but in contrast to that, the processes in the present case occur at an essentially lower temperature region, and then occur significantly faster.

Generally, the maximum of H_c characterizes the transition from firstly *superparamagnetic* micro-particles by increasing in size to 'mono-domain' particles with stable magnetization, which finally grow into 'multi-domain' particles with a *Bloch*-wall-structure, which leads to a decrease of H_c [56,57].

For a further proof of this conception in the present case of a hydride decay, the size- and field-strength-distribution of the *Barkhausen*-discontinuities, caused by irreversible *Bloch* wall displacements, was investigated during the desorption of hydrogen [57]. The Barkhausen-discontinuities ('jumps' resp.), which are discontinuous changes of the magnetization during a continuous change of the magnetic field, induce voltage impulses in a coil surrounding the sample, which are proportional to the change of the magnetic moment of the sample. An electronic measuring device allowed to record the number and the time slope of the Barkhausen-impulses during alternating magnetization, as well as the size distribution of the jumps. The quantity to be measured may be explained by Fig. 5 [57–59].

If a sample becomes magnetized along one branch of the hysteresis loop, the Barkhausen-jumps preferentially arise at its steep part. The number of jumps per field strength unit approximately has the course presented below. The maximum of the critical field strength HK need not coincide with the coercitivity H_c. The area below this curve is proportional to the total number of the Barkhausen-jumps. The sensitivity of this measuring device allowed to detect jumps with a magnetic moment greater than $5.8\times10^{-9}\ \mathrm{A\cdot m^2}$.

The presented investigations were made at cathodically hydrogenated [6] nickel foil samples of a thickness of $6\,\mu$m. In Fig. 6 [57] the time slopes of the saturation magnetization I_s and of the Barkhausen-jump-number n during the desorption of the hydrogen at room temperature are plotted. At the beginning, *i.e.* at optimal (at an atomic ratio H/Ni > 0.7) hydrogenated nickel, I_s is practically zero, and at first increases fast, then slowly and after about 10 hours reaches the value of pure nickel. In contrast to

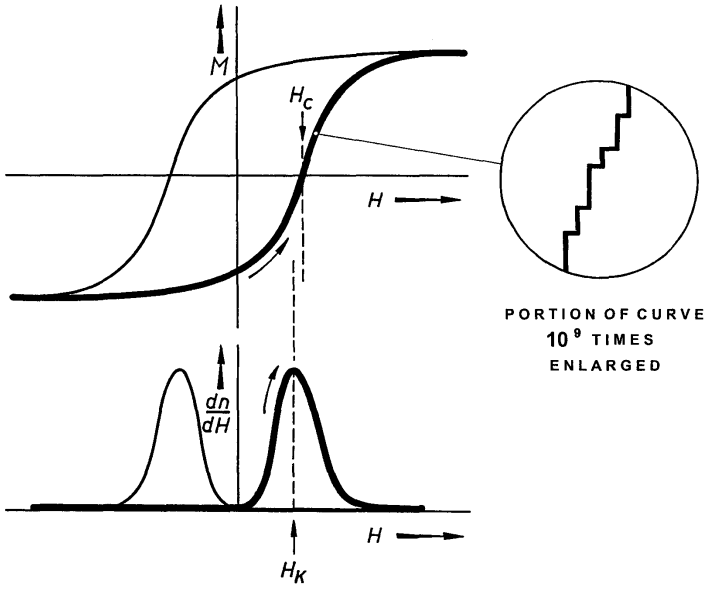

Figure 5. For explanation of the quantity to be measured (schematic). – Above: hysteresis loop. – Below: jump number per field strength unit as function of field strength.

this, the start of the Barkhausen-jumps is delayed: in the present case *ca*. 100 min before the first jump of the above-mentioned size arose, although within this time I_s had already rosen to 30% of its maximal value, *i.e*. 30% of the material had already become ferromagnetic. In the further course, the number of jumps strongly increases, passes a maximum and then decreases fast, whereby the value of the uncharged sample with $n_o = 20070$ is not reached again.

The *size distribution* of the Barkhausen-jumps in the different states of desorption, as well as those of the uncharged sample, are presented in Fig. 7 [57]. It is significant to see that at the beginning of the decay of the nickel hydride, only small jumps arise, bigger ones take place only later; the values of the uncharged sample are not reached again.

The delay of Barkhausen-jumps at the decay of the nickel hydride, as well as the increase of the mean jump size during the desorption of the hydrogen, can be explained by the formation and the growth of small ferromagnetic particles in a non-ferromagnetic matrix. Below the starting point of the Barkhausen-jumps, this tendency indicates the existence of ferromagnetic particles with a volume of about $v = 10^{-9}$ cm^3.

The fact is that the observed maximum of the jump number n of a ferromagnetic nickel phase, which is rebuilt at about 70%, can correspond to the beginning of the particles growing together as well to the observed decrease of H_c and H_k.

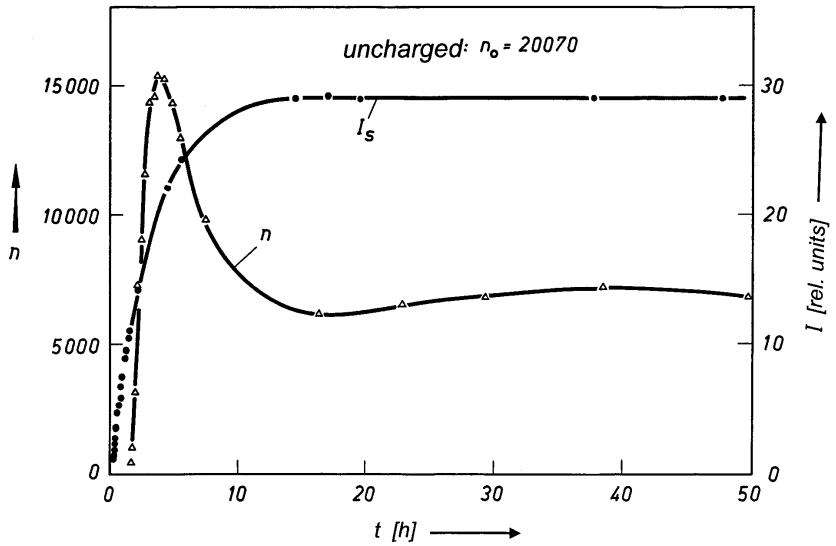

Figure 6. Time slope of the saturation magnetization I_s and the Barkhausen-jump number n during the desorption of the hydrogen at 20°C.

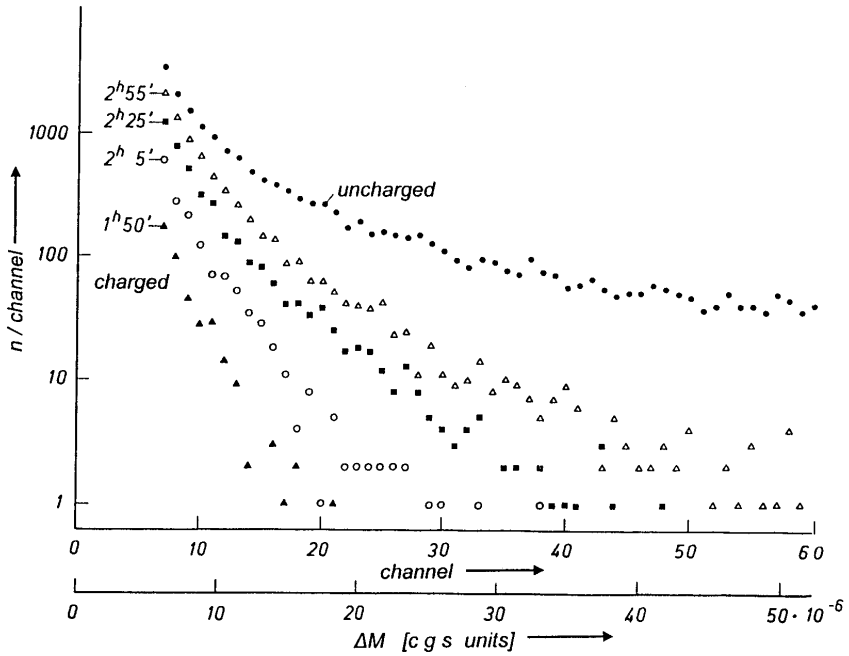

Figure 7. Curves of size distribution $n(M)$ of Barkhausen-jumps during the desorption of hydrogen at 20°C.

Altogether, the results support the conception of the decay of the nickel hydride, which is comparable to the precipitation of common alloys. This also suggests the following *metallographic* investigation: the transfer of a magnetic 'decoration technique' [39] responding to the coexistence of ferromagnetic and non-ferromagnetic regions – based on a modification of the well-known Bitter method according to Hutchinson *et al*. [70] and proved in a preceding paper [71] – permits the direct detection of the occurrence of the ferromagnetic α-phase precipitation (corresponding to the miscibility gap in the phase surface, Fig. 1) in a decomposing (non-ferromagnetic) hydride or NiH_β – matrix resp. Here, by the settlement of small ferromagnetic iron particles produced by evaporation in argon atmosphere and attracted by the magnetic stray field of the sample surface, which finally can be observed at the respective spots in an optical microscope as blackenings ('Bitter powder pattern'), the dispersed nature of the α-phase precipitations, clearly identified by their ferromagnetism, is made visible: Fig. 8.

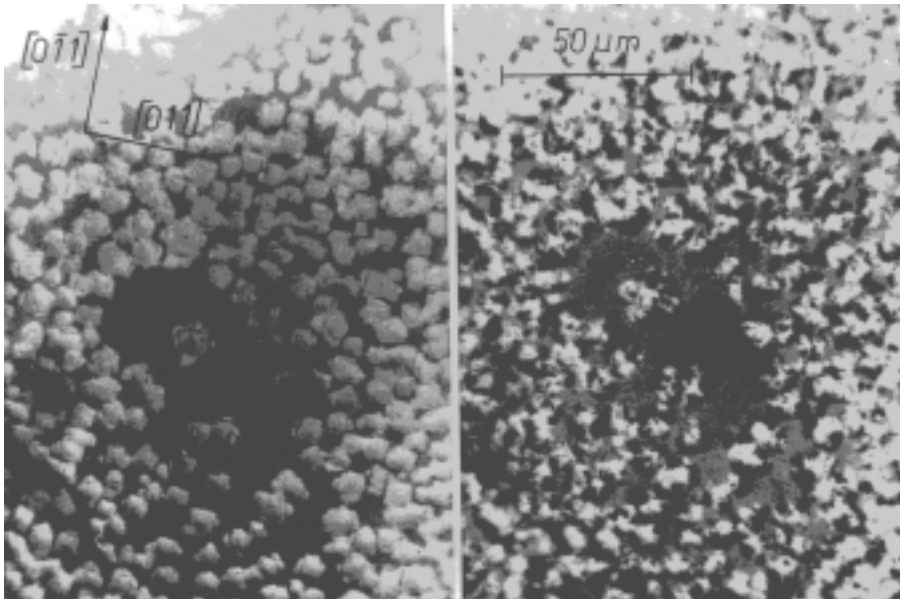

Figure 8. Detection of α-phase precipitations in decomposing NiH_β by 'Bitter powder pattern'. The optical micrographs are showing the same part of the (100) – surface in only slightly different $\alpha+\beta$-states of desorption of β-NiH; (a) before, and (b) after decoration with iron particles, [39].

This example may generally show the usefulness of these methods of 'visualization' for analysing of local particularities of phase transitions in metal-hydrogen systems with ferromagnetic components, especially in the two-phase region of the phase surface, Fig. 1.

The results from the Ni-H system, as well as the analogous behaviour of the palladium-hydrogen system, suggest a comparison with the corresponding substitutional alloys – according to the displacement rule, thus, with nickel-copper or palladium-silver resp. As at cathodic formation of Ni-H_β, also in case of ferromagnetic nic-

kel-copper alloys, it is possible to follow the hydrogen *absorption* magnetically, due to the cancellation of the spontaneous magnetization by interstitial hydrogenation, whereby one can also suggest that the hydrogen progresses in a more or less frontal shape from the sample surfaces. Thus, the magnetization curves of the (annealed) foils of Ni and Ni-Cu in Fig. 9, [36] (as in Fig. 2) represent the decrease of the magnetic regions between the hydride fronts up to the non-ferromagnetic state, evidencing the complete pervasion of the sample material with hydrogen. One can recognize the significant increase of the penetration velocity of the hydrogen with increasing Cu-content, which is also connected with the enlarged lattice parameter, caused by the copper presence [35,36].

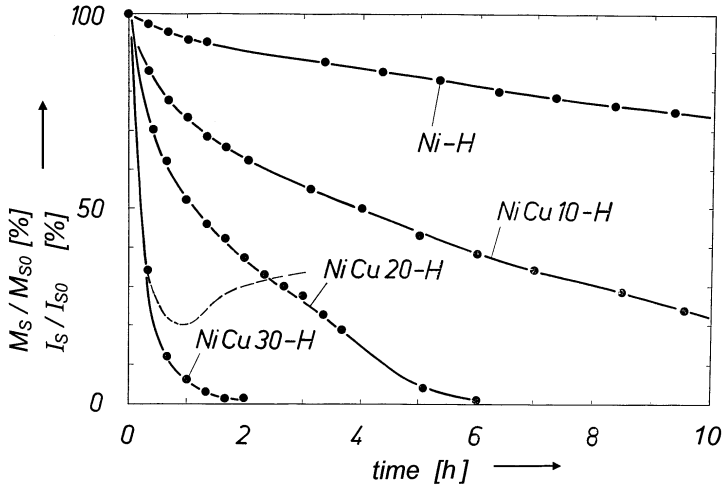

Figure 9. Decrease of the saturation magnetization M_S of nickel and nickel-copper foils (of 20 μm thickness) during cathodic absorption of hydrogen at 20°C. M_S saturation magnetization of the uncharged samples. (Dashed line: example for diminished hydrogen absorption in case of first charging of unannealed material) [36].

The decomposition process of the hydrides and so the desorption velocity of the hydrogen is, in a complicated manner, dependent on the preliminary treatment of the material (incl. repeated hydride forming and decomposition cycles), which is reflected in the time course of the restoring magnetization as well as in the eudiometrically determined amount of the hydrogen desorbed in the respective time. In contrast to the clearer behaviour of the absorption, the desorption process is not yet completely clarified[2].

[2] Possibly X-ray findings play a part for the fact that many samples show weak copper-lines, which point to Cu-segregations [36,37]. – Especially, in case of repeated hydrogenation cycles ('training') the surfaces of sample foils with higher Cu-contents showed a reddish discolouring, perhaps also as an indication for a preferred transport of copper atoms in the main hydrogen desorption direction (H.J.B.).

In spite of the variety of the appearances in all cases – independent of the mentioned preliminary treatment and contrary to the respective amount of desorbed hydrogen – a time lag behind of the returning magnetization could be observed in [36], which corresponds to an 'overcharge-part'.

The expansion of the nickel lattice by interstitial hydrogen [15], mentioned at the beginning, of course suggested corresponding studies at the alloys of nickel. In this sense X-ray investigations at the Ni-Cu-H system have been started by B. Baranowski and S. Majchrzak [35], and at Munich University as well [29]. The results of both groups are in agreement and show the correspondence of the behaviour of the Ni-Cu-H alloys with that of the system Pd-Ag-H [72] keeping the *fcc* lattice.

The mentioned occurrence shown of an 'overcharge-part' connected with hydrogenation is – as to be seen in Fig. 10a – also reflected in the course of the lattice parameters of the system Ni-H during the desorption of the hydrogen: The continuous sloping down of the first part of the curve corresponds to the reduction of the oversaturation of the hydride-rich β-phase with atomic ratios $1.0 > n_H/n_{Ni} \geq 0.6$[3].

This appearance of an additional – continuous – lattice expansion is also known at the system Pd-H [72].

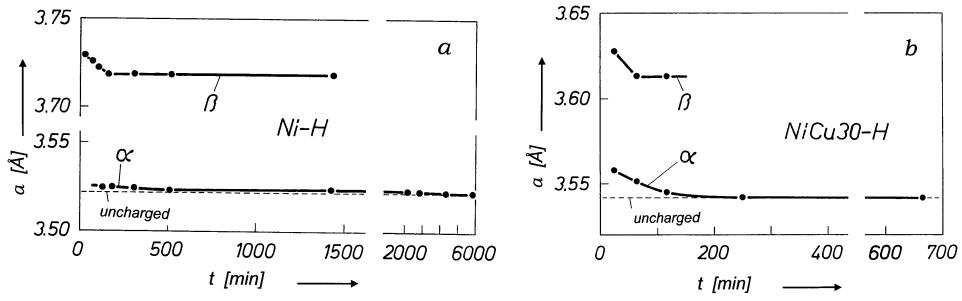

Figure 10. Lattice parameters of the systems Ni-H and Ni30at%Cu-H during desorption of the hydrogen at 30°C [36].

In the same way the α-phase presents itself as an only slightly pronounced lattice expansion, decreasing continuously with the desorption time. But for pure nickel it cannot be decided clearly if the lattice widening at the α-phase is directly caused by hydrogen solved in low concentration or by strain around still existing β-phase regions. Findings about the coexistence of α- and β-phases at the system Ni-H are reported in [33].

Fig. 10b shows an example for the similar behaviour of the Ni-Cu-H system found at 10, 20, 30 and 35 at % Cu content: the maximal lattice expansion of the α-phase in-

[3] A correlation with electron diffraction results in [16] about a larger lattice parameter at the surface of the Ni-H system as compared to bulk Ni-H cannot be excluded.

creases with growing Cu-content, whereas the stationary lattice expansion of the β-phase is diminished.

As shown in Fig. 11, a simultaneous presentation of the measured lattice expansion Δa (without over-charging) and the atomic ratio n_H/N ($N = n_{Ni} + n_{Cu}$) *vs*. copper content of the samples is of particular interest, whereby of course the n_H/N values still contain the over-charge part (for two pre-treatment cases): thus, also the hydrogen inserted additionally, after the formation of the β-phase – similar to the behaviour of disordered mixed isomorphic crystals – causes a further continuous lattice expansion as in Fig. 10. The fact alone, that inspite of different pre-treatments of the material the hydrogen solubility decreases to a Cu-content of about 60 at% indicates the correlation with a respective number of empty states in the d-band.

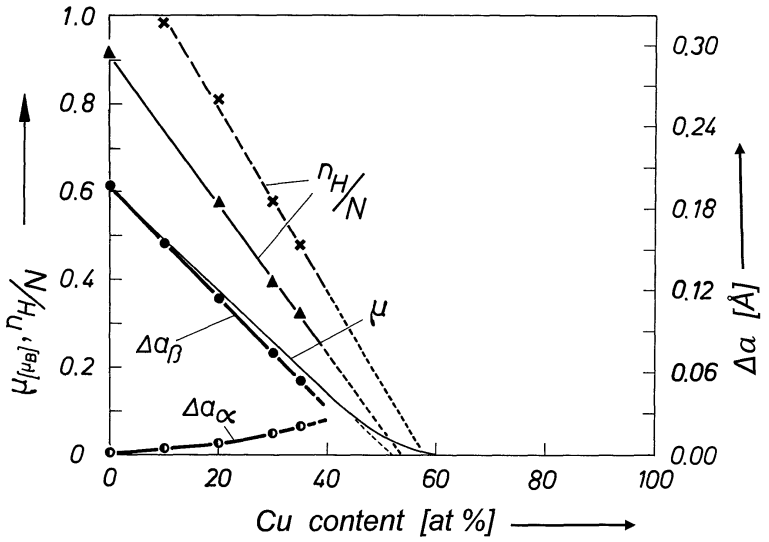

Figure 11. Atomic ratio n_H/N and lattice expansion Δa of NiCu-phases at 20°C. n_H, N quantity of hydrogen – resp. alloy-atoms. **x** annealed, ▲ unannealed but 'trained'. μ means magnetic moment per atom (cit. in [36]).

From the equality of the numerical value of n_H/N of the stationary β-phase at the NiCu-alloys and of the mean magnetic moment μ(NiCu) per atom (measured in Bohr magnetons) and on the other side from the validity of the Vegard's law proportional to the lattice expansion Δa follows

$$\Delta a(NiCu) = const \cdot \mu(NiCu) \tag{3}$$

That means, that the H-concentration of the (non-oversaturated) β-phase corresponds to the respective d-band filling.

For an exact knowledge of the correlation between the cancellation of the spontaneous magnetization and the hydrogen concentration needed for it, the production of a homogeneous non-ferromagnetic hydride phase is an important precondition for a controlled decomposition process, as well as for the determination of both the maximal amount of the interstitial hydrogen in the regular octahedral sites and that *minimal* amount, required for cancelling the magnetic moment of the host. For this, instead of electrochemical methods [6], the application of high pressure gaseous hydrogen was chosen [23,52]. With values above 1 GPa, which exceed the respective hydride formation pressure, an atomic ratio $n_H/n_{Me} = 1$ could nearly be attained in all cases, which corresponds to an occupation of all octahedral sites of the fcc lattice with hydrogen, see Fig. 12 [76]: The decomposition of the hydrides (performed stepwise on a set of samples because of the mass-spectroscopic analysis) monitors the release of hydrogen from the octahedral sites and the emptying of d-holes, which is reflected in the rising values of M_S measured at 4 K.

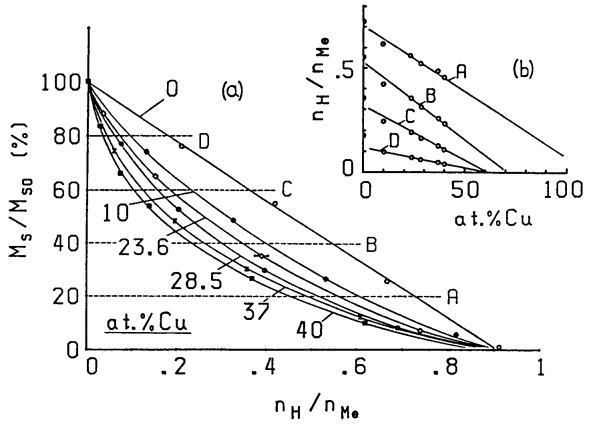

Figure 12. Correlation between saturation magnetization M_S at 4 K and hydrogen concentration, expressed by the mean atomic ratio n_H/n_{Me} for Ni and different Ni-Cu alloys. (M_{SO} saturation magnetization before hydrogenation. Each measuring point represents a separate sample. Mean sample thickness: 12 μm). Curves A,B,C,D in the insert obtained from the corresponding intersection points of the horizontal dashed lines with the measuring curves in the figure show the n_H/n_{Me} values of the Ni-Cu alloys *vs*. alloy degree for successive decomposition stages of the corresponding hydrides, which are characterized by the same M_S/M_{SO} of the restored ferromagnetism. Curve D of the insert shows the minimal H required for cancelling the magnetic moment of the different Ni-Cu alloys considered for the case of a restored ferromagnetism of $M_S/M_{SO} = 0.8$ [76].

The graphs in Fig. 12 show that the hydrogen concentration, needed for a reduction of the respective magnetic moment equivalent for all alloys, decreases approximately linearily with increasing Cu-content. Here, especially at the curves C and D, which represent stages with an extensive removed overcharge-part, at a Cu-content of 60 at% the value zero is reached. That is a significant indication of the parallelism between hydrogen insertion and the occupation of empty states in the 3d-band (at 60 at%

Cu the d-holes of nickel are completely filled up [29]). This minimal atomic ratio of $n_H/n_{Me} = 0.6 \pm 0.1$ could also be obtained by neutron-diffraction measurements [17].

As a further example for dealing with this complex of questions, the ferromagnetic alloys of nickel with chromium of 2 to 7 at % were chosen [38]. They also absorb hydrogen in high concentrations, followed eudiometrically, until they form a β-phase, and they loose their ferromagnetism by interstitial hydrogenation, combined with reversibly enlarged lattice parameters of some percent – decreasing with increasing Cr-content.

The variation of the lattice expansion Δa with Cr-content is, in some way, similar to the proportionality of Δa with the mean magnetic moment, found in case of Ni-Cu-hydrogen alloys, but deviates in a characteristic manner. Possibly this is due to the fact that chromium has only a half-filled d-shell.

X-ray investigations also showed an additional increase of Δa by supersaturation of the β-phase and the occurrence of a second phase with very low values of Δa (for details see [38]).

4. ^{57}Fe Mössbauer spectroscopy on nickel-based hydrides*

For winning further insight into the microscopic structure and processes of nickel-based hydrides and its formation, the Mössbauer spectroscopy has been integrated in the investigations. Mössbauer studies on dilute substitutional iron in electrochemically hydrogenated nickel have shown, that the electron density at the iron nuclei is reduced by hydrogenation [78,79,80]. Concerning the question of the influence of the degree of occupation of interstitial sites by the hydrogen, the Mössbauer investigations on electrochemically produced hydrides have in addition also been extended to those won by application of high pressure gaseous hydrogen [81].

Fig. A shows some typical Mössbauer spectra. The electrolytically loaded sample still contains 15% of the magnetic α-phase. From the mean hydrogen content H/metal ratio of $\bar{x} = 0.87$ one estimates $x = 1.02$ β-phase fraction. The pressure-loaded sample with $x = 1.02$ consists of the pure β-phase. The spectra were interpreted in the same manner, as has been successful for ^{57}Fe in β-PdH_x [82–85], *i.e.*, by assuming that the quadrupole interactions are negligibly small, and that the isomer shift increases linearly with the number i of nearest neighbours surrounding a Mössbauer atom, but else do not noticeably depend on the hydrogen content. Like in the case of PdH_x, the main support for the crucial assumption that quadrupole interactions can be disregarded stems from the spectra measured in external magnetic fields [81].

The analysis of Mössbauer spectra of dilute ^{57}Fe probes in nickel hydrides shows that it depends on the method of preparation and on temperature [81]. The spectra show that iron in β-NiH_x ($x \approx 1$) interacts repulsively with hydrogen in a similar manner as in palladium hydride [82–85].

*Special indication of figures (A, B) in this section.

Consequently the number of hydrogen atoms next to the probes increases with increasing temperature, as the repulsive interaction is overcome by thermal activation. The hydrogen environment, existing near room temperature, can be frozen in by rapid quenching. The relaxation of such non-equilibrium states towards equilibrium was observed between 130 and 150 K in isochronal and isothermal annealing experiments [86].

So the Mössbauer experiments detected at the surface a mobility of the hydrogen already at these low temperatures [86]. This reflects an important difference between the two systems, due to the relatively slow diffusion of hydrogen in NiH_β and this renders relaxation effects not seen in the Pd case, observable in nickel hydride [86].

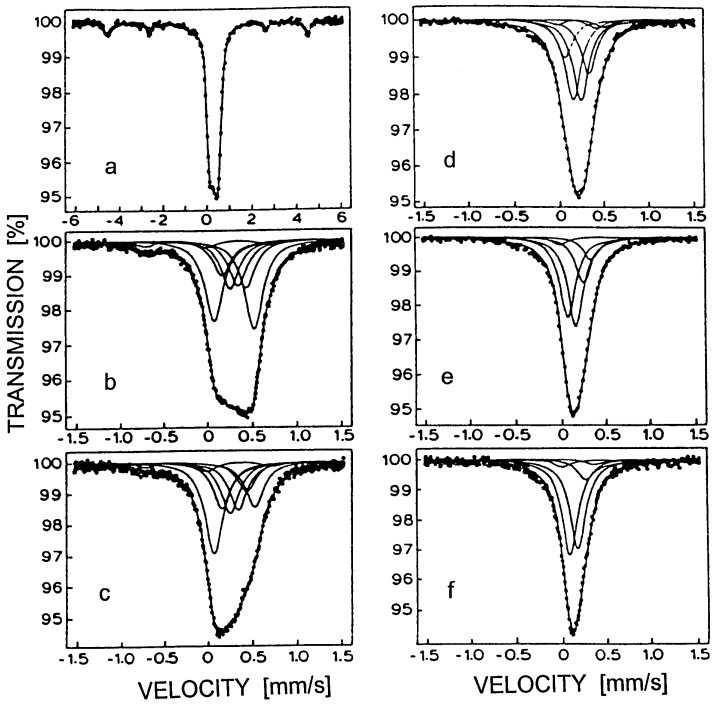

Figure A. Mössbauer spectra of ^{57}Fe in Ni hydrogenated electrolytically (left) and under high pressure (right). Spectrum (a), taken at 75 K, represents an as-quenched NiH_x sample with a mean hydrogen content of $x = 0.87$, which still contains 15% of the magnetic phase. All other spectra were measured at 100 K. Spectrum (b) is again a as-quenched sample measured with a smaller velocity to show the structure of the hydride pattern. Spectrum (c) was taken after the sample had been at 150 K for 24 h. The leftmost of the fitted Lorentzian components corresponds to 0, the rightmost to 6 hydrogen neighbours. Spectrum (d) is of an as-quenched pressure loaded $NiH_{1.02}$ sample, (e) and (f) are for the same sample after annealing at 150 K for 1 h and 24 h, respectively. The ^{57}Co:Rh source was always at 300 K.

The strong repulsion of the hydrogen, especially by the iron at hydrogen-to-metal ratios very close to unity, motivated Mössbauer studies on hydrides, such as those of Ni-Cu alloys [88]: in this case the distribution of hydrogen around the iron probes is expected to be changed to an other element.

Owing to corresponding experiments, the hydrogen-induced isomer centre shifts for ^{57}Fe in $Ni_{0.7}Cu_{0.3}H_x$ show a strongly non-linear dependence on the hydrogen content, but are generally higher than those for Fe in hydrides of pure nickel [89], Fig. B, where below room temperature the non-ferromagnetic β-phase exists only with hydrogen contents $x \geq 0.9$ [83,88].

The shifts for β-NiH_x show no correlation with the hydrogen content. Such a steep increase is expected, if there is a strongly repulsive interaction between the hydrogen and the iron probes, which largely prevents hydrogen from occupying sites next to iron atoms, except at hydrogen contents close to $x = 1$.

For the $Ni_{0.7}Cu_{0.3}$ alloys (showing no ferromagnetism at hydrogen-to-metal ratios above $x \approx 0.3$), the increase of the isomer shift with the hydrogen concentration is smoother, indicating that hydrogen penetrates into the vicinity of the iron probes already at lower hydrogen concentrations. This can be explained by a distribution of interstitial site energies in the disordered Ni-Cu alloys, where interstitial sites with many Cu neighbours will be less favourable for hydrogen occupation than sites with fewer or none.

Hydrogen sites with an iron neighbour will be distributed within the range of site energies and, therefore, together with other sites, gradually become filled with comparable energy. The lack of sensitivity of the ^{57}Fe for probing the influence of the dis-

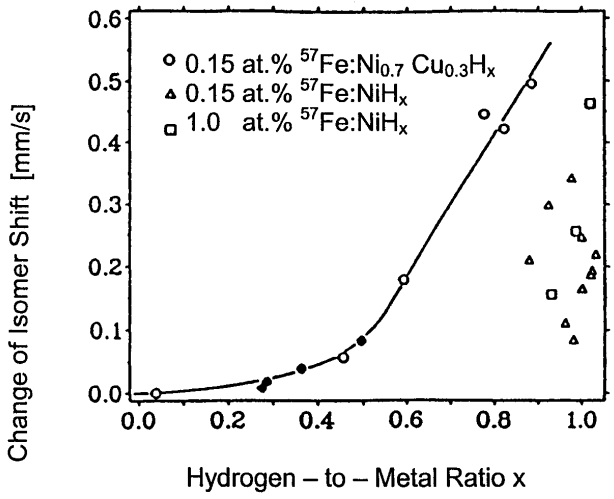

Figure B. Isomer shifts of the ^{57}Fe in $Ni_{0.7}Cu_{0.3}H_x$ hydrides as a function of the hydride content. Open circles represent data from single phase, filled circles data from two-phase specimens. The shifts were measured at 100 K and are given relative to hydrogen-free $Ni_{0.7}Cu_{0.3}$ at the same temperature. Shifts for dilute ^{57}Fe in NiH_x hydrides with respect to unloaded nickel are shown for comparison (triangles and squares).

solved hydrogen in the α-phase can also be understood in this way, since for small x the interstitial sites next to the iron will not be occupied even in Ni-Cu alloys.

Mössbauer spectroscopy can, thus, be used as a sensitive tool for studying details of the microstructure of hydrides of *e.g.* nickel-based alloys and among them those, which cannot be distinguished by only (ferro)magnetic measuring methods.

5. Magnetothermal analysis of hydride decomposition processes of ferromagnetic metal-hydrogen systems in analogy to that applied in the case of common alloys

As mentioned before, earlier research also revealed a magnetic behaviour in the regarded metal-hydrogen systems, known from common alloys. This suggests the transfer of methods, well proved at evaluations of magnetic behaviour for constitution analysis of common alloys, to ferromagnetic metal-hydrogen systems, showing a similar behaviour.

In this sense we here regard deviations of the temperature dependence of the saturation magnetization $M_S(T)$ – including the Curie temperature – from the ideal M_S-T-curve occurring at metal-hydrogen systems already at normal conditions during the decomposition of initially non-ferromagnetic hydrides.

Shape changes of the M_S-T-curve at common alloys, as of nickel with gold or beryllium resp. as a consequence of precipitations caused by heat treatment, were used by W. Gerlach for the development of a method of 'magnetothermal analysis' for the constitution of alloy systems [92].

The fact, that at our hydride systems the interstitial insertion of the hydrogen is accompanied by a large lattice expansion (in case of nickel about 6% [15]), leads to considerable changes in the matrix during hydrogen displacements, quite in correspondence with metallurgical processes in common alloys.

This correspondence finds its expression in the shape of the 'temperature dependence of the saturation magnetization' $M_S(T)$ – including the Curie temperature – well-known as a characteristic for the constitution of an alloy [92–95].

In analogy to common alloy systems, we can conceive the reappearance of the arising ferromagnetic phase – which is accompanied by hydrogen desorption – within the metal-hydrogen system (resp. hydride) as a 'precipitation process' [66–69]. It causes an inhomogeneous distribution of hydrogen within both the non-ferromagnetic hydrogen-rich (β-) phase and the ferromagnetic hydrogen-poor (α-) phase. (Whereby *e.g.* the atomic ratio n_H/n_{Ni} for Ni-H_β is about 0.6, and for Ni-H_α up to about 0.03 [6].) Therefore, it can be expected that the local variations in the distribution of the dissolved hydrogen change during the hydride decomposition process. This is confirmed by the changes of the shape of the M_S-T-curves, observed at different hydride decomposition stages and it reflects the corresponding changes of the 'hydrogen concentration spectrum' in the samples investigated.

These observations suggested to take up the above-mentioned method of a 'magnetothermal analysis'. This method has turned out to be significant for the analysis of the constitution of common alloys and we have transferred and extended it to ferro-

magnetic metal-hydrogen systems showing, as mentioned, a similar behaviour [33,96]. The shape changes of the M_S-T-curves, which are induced by the hydrogen, can – in analogy to common alloys – be regarded as consequences of a superposition of M_S-T-curves of regions of different hydrogen concentrations c_H, arising 'precipitation-like' within the hydride matrix. See *e.g.* the scheme, Fig. 13 [97,98], of the M_S-T-curves of an alloy containing four ferromagnetic phases with different concentrations (and different Curie temperatures), but each phase being homogeneous. Of course, one can extend these considerations to Me-H systems with more phases and finally generalize them for a heterogeneous alloy with a more or less continuous distribution of the dissolved alloy component hydrogen.

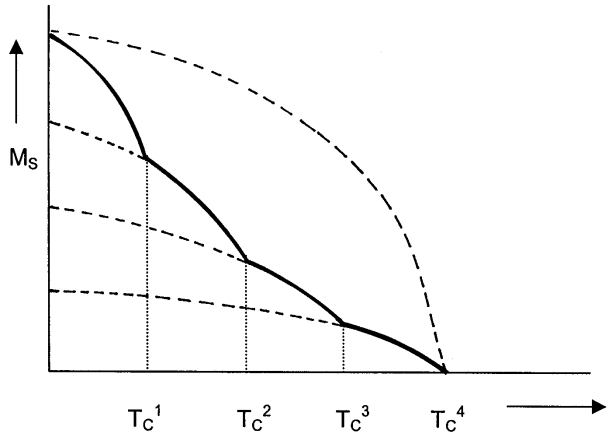

Figure 13. Scheme of the M_S-T-curve of a heterogeneous alloy, containing four homogeneous ferromagnetic phases. Each of the dashed curves represents an ideal M_S-T-curve, which characterizes homogeneous ferromagnetic systems. T_c^j: corresponding Curie temperatures.

On the corresponding assumption, now in the sense of the '*Law of corresponding states*' that for all homogeneous regions of different hydrogen concentrations the reduced magnetization $M_S(T)/M_S(0)$ is a unique function of the reduced temperature T/T_c^j – with T_c^j meaning the Curie temperature at hydrogen concentration c_H^j – the distribution of the hydrogen concentration for different stages of hydride decomposition can be calculated. The 'magnetothermal analysis' – well proved in common alloys [92–95] – is here demonstrated on metal-hydrogen systems, based on alloys of nickel with copper and chromium [76,96–98].

The endeavour to draw upon the ferromagnetic characteristic of the considered metal-hydrogen systems for analysis of the metallurgical role of the interstitial hydrogen, required the employment of special techniques of measurements and in addition of high sensitivity, as both at the final stages of the hydride formation and in the initial stages of the hydride decomposition, all kinds of small magnetic effective cross sections exist.

For this purpose a highly sensitive microcomputer-controlled AC magnetometer with a phase-locked data acquisition system was developed for measurements in applied fields up to 3×10^5 Am^{-1} [99]. It works on the basis of the 'Signal-Averaging-Method', which besides a high resolution also delivers the required high density of measured data. This measurement technique allows to extract a measuring signal at first totally hidden in noise of any quality from the noisy background. For the illustration of the power, offered by the AC magnetometer – especially of its usefulness for the detection of precipitation processes in ferromagnetic metal-hydrogen systems – see Fig. 14 [99].

In order to ensure the total hydrogenation of the whole sample volume, the samples absorbed hydrogen under high hydrogen pressures in GPa-range, well above the formation pressure of the respective hydride. Furthermore, alloys were chosen with Curie temperatures below the decomposition temperatures of the corresponding hydrides at normal pressure (about 0°C). The hydride decomposition was performed in steps near 0°C at normal pressure: the M_S-T curves were obtained by interrupting the hydrogen desorption by freezing the sample, measuring the respective M_S-T curve and continuing the hydride decomposition after warming up the sample to nearly 0°C.

Measurements of the temperature dependence of the saturation magnetization $M_S(T)$ of the systems Ni-7at%Cr-H and Ni-40at%Cr-H, as performed by the above-mentioned AC magnetometer, are presented in Figs. 15 and 16 [76,97,98]. One can see that, dependent on the respective alloy and because of the high mobility of the hydrogen by stepwise short-term desorption (in the order of minutes), already at room temperature partly *drastic* deviations of the M_S-T-curve from that of the hydrogen-free state can be produced, which is particularly true here for Ni-40at%Cu-H by flattening (respectively sagging) of the M_S-T-curve – corresponding to a wide spectrum of different Curie temperatures. Similar changes of the shape of the M_S-T-curve are, as mentioned above, well-known at common alloys as typical precipitation effects, where, however, migration of matrix atoms needs higher temperatures. In the present case the appearances are caused by different distributions of hydrogen in the different materials and decomposition states respectively.

In order to receive from such measurements information about the distribution of hydrogen, the aforementioned method of magnetothermal analysis was applied, yielding the histograms presented in Fig. 17, which are calculated from the measured data of Figs. 15 and 16.

The sequence of histograms in Fig. 17 – here to be read from back to front, according to decreasing hydrogen content – illustrates the stepwise transition from the non-ferromagnetic hydride state 1 (here $c_H/c_H^{max} = 1$ is valid for the whole sample, *i.e.* $\Delta V(c_H^{max})/V = 1$) to the finally hydrogen-free ferromagnetic state (here $c_H/c_H^{max} = 0$ is valid for the whole sample, *i.e.* $\Delta V(c_H = 0)/V = 1$). This means, that during the decomposition of the hydride, the relative volume fraction $\Delta V(c_H = 0)/V$ of the ferromagnetic hydrogen-free state (left hand of the histograms) grows at the cost of the (decreasing) relative volume fraction $\Delta V(c_H^{max})/V$ of the non-ferromagnetic hydride state (right hand of the histograms). The sequence of volume fractions between these

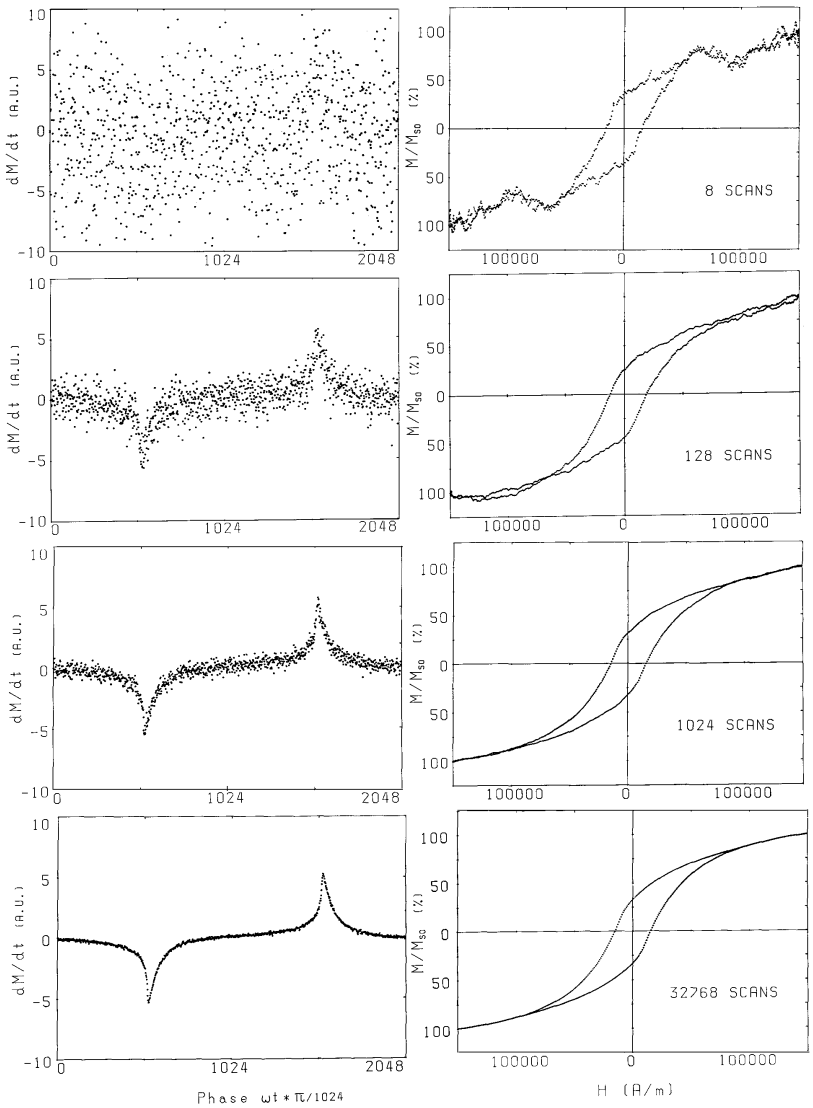

Figure 14. Both sequences of computer plots show records of an extremely weak magnetization signal dM/dt covered by the noise effect at the beginning and measured at an almost completely hydrogenated 4 μm thick nickel foil sample with remaining ferromagnetic cross section of only 5×10^{-5} mm^2, and of the corresponding hysteresis loop M(H). The plots demonstrate the high density of data points and the large improvement in signal-to-noise ratio as a consequence of the increasing number (8, 128, 1.024, and finally 32.768) of signal averaging scans. Note that the signal emerging from noise and the shape of the corresponding hysteresis loop becoming more and more perfect with increasing number of scans.

extreme states characterizes the individual spectral distribution of the hydrogen concentration in the different samples or sample states. Of course, this presentation contains no information about the spatial distribution of the hydrogen within the sample.

Such concentration spectra allow conclusions concerning the phase diagram of these systems (Fig. 1): Thus, the calculated distributions of hydrogen concentration in the case of Ni-7at%Cr-H show that the decomposition of the hydride at room temperature by β-α-phase transition occurs in the heterogeneous two-phase-region, *i.e.* below the critical temperature of α-β-phase separation. From the absence of a mixing gap at Ni-40at%Cu-H, however, it can be concluded that the hydride decomposition at room temperature, combined with hydrogen desorption, occurs above the critical point of β-α-phase separation, the critical temperature being at or below 1000 K (corresponding results on the systems Ni-9at%V-H and Ni-10at%Ti-H as examples for $\beta \rightarrow \alpha$ phase transition near resp. below the critical point of $\beta \rightarrow \alpha$ phase separation are presented in [98]).

An analogous proceeding at different hydride decomposition temperatures and different degrees of alloying of the metal matrix allows to probe the phase diagrams of the corresponding metal-hydrogen systems. Here, for the sake of maintaining the stability of these systems up to temperatures in the region of the respective Curie temperatures, the application of high pressure hydrogen gas is needed. Some corresponding results are subject of the following section.

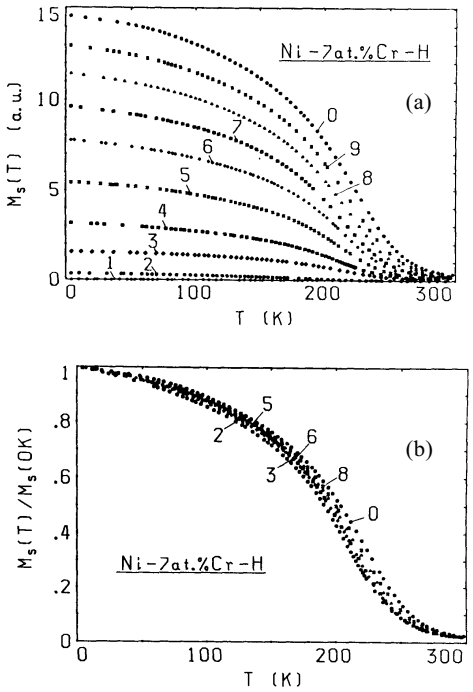

Figure 15. Sequence of measured curves of the saturation magnetization M_S as a function of temperature $M_S(T)$ for different decomposition stages (2–9 and 0) of an initially (curve 1) non-ferromagnetic Ni-7at%Cr hydride, (a) on arbitrary scale, (b) on a normalized scale. (Curve 0 – same as measured before hydrogenation; in (b) curve 1 omitted. Sample thickness: about 15 μm) – Note the uniform rise of the M_S-T-curves, which is a characteristic feature of a 'heterogeneous' precipitation.

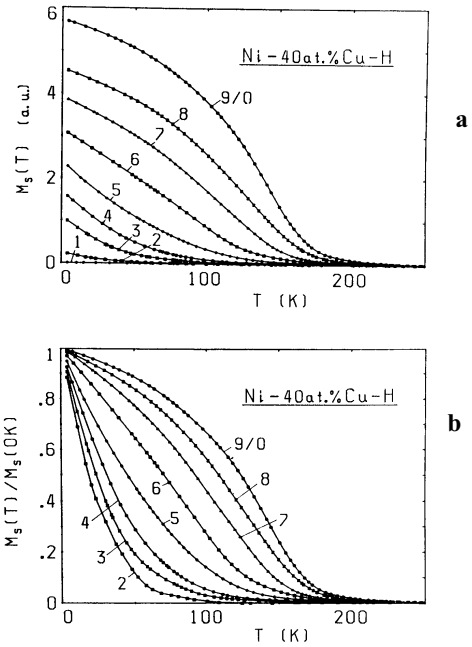

Figure 16. Stepwise decomposition of a non-ferromagnetic Ni-40at%Cu hydride. Corresponding to Fig. 15, (a) M_S-T-curves, (b) normalized scale. (Curve 0 – before hydrogenation; in (b) curve 1 is omitted. Sample thickness: about 12 μm) – Contrary to Fig. 15 here the M_S-T-curves show drastic variations in shape, indicating the predominance of a 'homogeneous' precipitation.

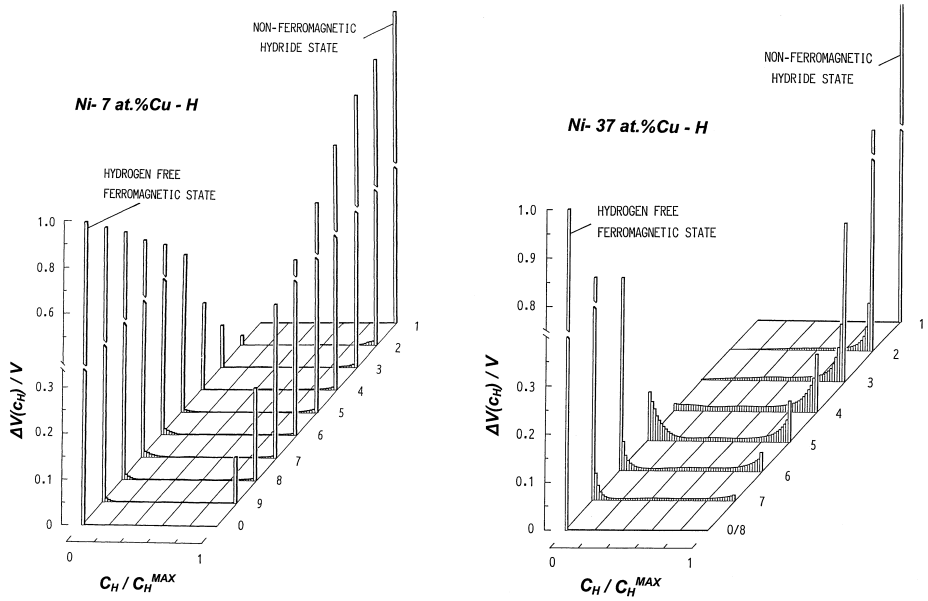

Figure 17. Sequence of histograms, which show the volume fraction $\Delta V/V$ with a certain hydrogen concentration c_H versus $c_H/c_H^{\max}$ for the different decomposition stages (1–9) of Ni-7at%Cr hydride and of Ni-40at%Cu hydride calculated from the measured data of Figs. 15 and 16 ($c_H^{\max}$: H content, necessary for cancelling the ferromagnetism of the sample).

6. Investigations on nickel and nickel alloys hydrogenated in high pressure gaseous hydrogen

A survey of metal-hydrogen systems in high pressure range and of the corresponding high pressure technique is given in some reviews [2,3,4]. This section gives an account of experiments performed in cooperation with B. Baranowski in Warsaw.

Further exploration of the above-mentioned instability of these nickel-based alloy-hydrogen systems, observed already near room temperature, requires the application of high pressure hydrogen in order to cover, to some extent, the phase surfaces. That is the only possibility for an extension of the investigations to higher (as well as to lower) temperatures and in many cases also for the preparation of metal-hydrogen systems resp. hydrides with components of the VI. to VIII. group of the transition metals. (See also the research work of the Russian group, cited in section 2).

Thus, at the presented alloys of nickel with Cr or with Fe, a complete transformation into the hydride phase of only 10 μm thick samples is no more attainable in a cathodic way, already at a low percentage of these components. The high pressure method allows to maintain the controlled thermodynamic activity during an experiment to follow the hydride formation, as well as the decomposition without additional manipulation. Informative discontinuities in physical properties turn up with hydride formation and decomposition. The electrical resistance R, as a proved physical property for such studies, on the other hand is sensitive towards the manifold structural changes within the material during hydrogenation, so that it is desirable to have a further physical criterion. Because of the advantages discussed above, the saturation magnetization M_S is especially suitable.

Such an experimental goal arises, besides the necessary small working volume in high pressure devices and its inaccessibility for bringing in sufficient magnetic field strength and especially in the case of wanted high temperature, new technological problems as concerning current leads, sealings or heat capacity and heat conductivity, which, as well as the kinetic conditions in the metal-hydrogen system, determine the measuring time. Determinations *e.g.* of Curie temperatures CT require a more or less extended temperature region and, therefore, a sufficient stability of the system studied. This means that for a fast continuous feasible measuring process – without time loss – one has to avoid thermal involvement of the mass of the high pressure apparatus, as well as the application of external magnetic fields. As mentioned in section 2, these requirements led to the development of a miniaturized magnetometer with internal magnetic field supply [30,31,100,101]. The last type, realized with an inner heater [47,96,100,101], is explained in the following.

The principle of the miniaturized magnetometer, Fig. 18 [11,28], rests on producing an induction signal by moving the sample magnetized in the field of a permanent magnet (up to about 3 kOe resp. 2.4×10^5 A/m) out from a coil. The sample motion is carried out by a non-magnetic mechanism, based on the thermal expansion and contraction of a wire heated electrically and moving a lever, which carries an arrange-

ment of sample, thermocouple and heater (50 W), plugged in a tubular pyrophyllite holder of only 4.5 mm^3 volume. So the measuring process implies the movement of a volume element up to 600°C hot and of only 4.5 mm^3 in a high pressure hydrogen atmosphere up to about 25 kbar in a working volume of some 1000 mm^3, whereas the geometry of heat conductivity guarantees the exact measuring of the sample temperature and on the other hand provides the high pressure sealings remaining below 30°C.

In Fig. 19, a Ni-Fe alloy may serve to demonstrate the ability of the described 'miniature magnetometer' responding very quickly to high pressure changes in the hydrogen atmosphere [102]. Even relatively small pressure changes in hydrogen are indicated by a steep change in the magnetization cycles. At the alloy regarded, with 16 at% Fe content, the hydride formation pressure amounts to 14–15 kbar (1.4–1.5 GPa) [102] and on the right of Fig. 19 one can recognize the rapidity, with which the hydride phase under pressures above the hydride formation pressure forms and below the comparatively slow increase in the magnetization, indicating a slow decomposition of the hydride. Obviously 'in situ' magnetization measurements are a definite and direct way to determine the formation as well as decomposition pressures. Fig. 20 [103] shows a group of Ni alloys, which completely lose their magnetization in high pressure atmosphere, corresponding to an increasing formation pressure with increasing Fe content and inversely in the case of Mn. The *correspondence* of 'electrical resistance' and 'magnetization' is shown in the diagrams of Ni-Mn-H systems in Fig. 21, which represents values of equilibrium with the high pressure hydrogen environment [103]. The electrical resistance of monitoring samples, made of identical alloys placed near the magnetic device, was measured during the magnetic measurements *i.e.* simultaneously under the same conditions. Furtheron, we here have an example for a direct relation to the phase surface scheme in Fig. 1:

Below about 20 at% Mn content, a typical pressure hysteresis exists, representing the difference between formation and decomposition pressures, caused by the miscibility gap, whereby the phase transitions ($\alpha \rightarrow \beta, \beta \rightarrow \alpha$) occur *below* the 'critical point'. The alloys with higher Mn-contents show no pressure hysteresis, *i.e*. the phase transitions seem to occur in a reversible manner *above* the critical point. Furthermore, one can see, that in spite of a complete hydrogenation of the whole sample forming a solid solution, confirmed by X-ray analysis [105], the magnetization does not vanish completely, as a consequence of an increasing prominence of the ferromagnetic properties of manganese in the host lattice (cf. corresp. results at cathodic hydrogenation of Ni-Mn alloys [106]).

In the following figures some experiments on Ni-H, Ni-Fe-H, Ni-Cu-H and Ni-Mn-H systems are shown, which are extended to *higher temperatures.* They are performed with the miniature magnetometer, Fig. 18, and a corresponding device for resistance measurements.

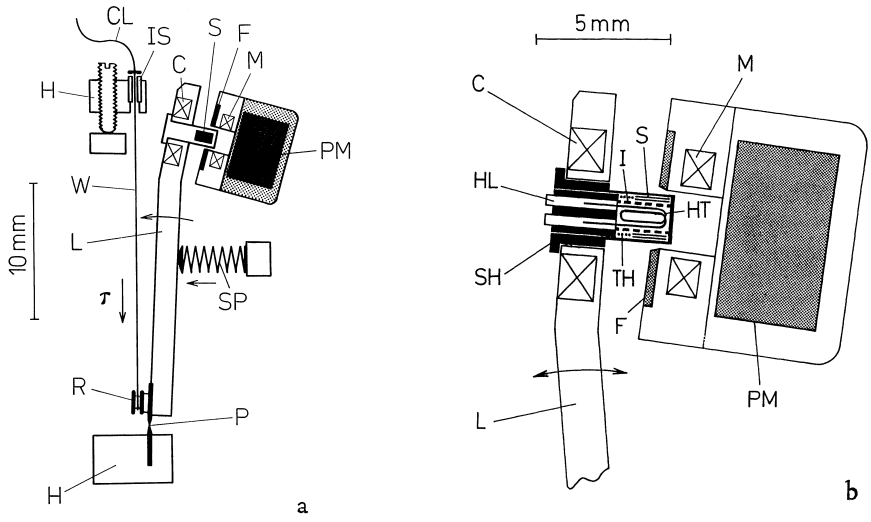

Figure 18. Scheme of the magnetic device: a) complete, b) enlarged part. S – sample, PM – permanent magnet (SmCoS: Brown, Boveri AG), F – magnetic flux piece, M – measuring induction coil, C – magnetic field control induction coil, L – lever, P – elastic pivot, SP – compression spring, H – holder, W – heating wire (looped around the insulating roller R), T – thermal dilatation of W, I – isolating tube, CL – current leads, SH – tubular sample holder, HT – sample heater, HL – heater leads, TH – thermocouple.

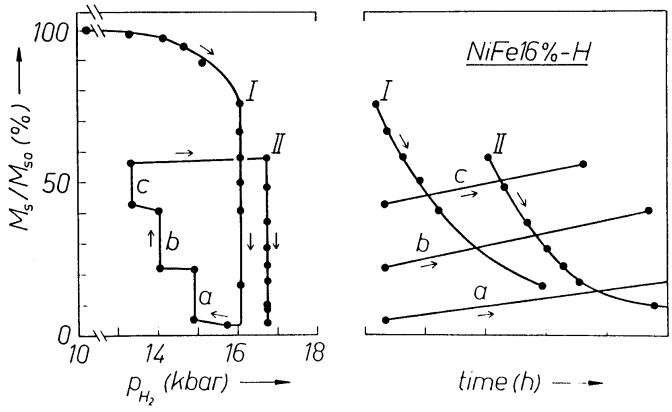

Figure 19. Relative saturation magnetization M_S/M_{SO} of a Ni-Fe alloy *versus* hydrogen pressure at about 22°C and the corresponding time sequence of the magnetization at different constant pressures (I, a, b, c, II). M_{SO} saturation magnetization at normal pressure (before hydrogen absorption).

The extension of the measurements to higher temperatures does not only serve for determining the Curie temperature *CT*, but also the informative shape of the temperature dependence of the saturation magnetization M_S, as well as of the electrical resistance *R*: The diagrams of M_S-*T* dependence in Fig. 22 and 23 show evident differences. Although the magnetism is annihilated in each case, after passing the corresponding for-

mation pressure of hydride (see *e.g.* Fig. 20), H desorption (by pressure reduction or heating) leads to different shapes of the M_S-T-curves. For Ni (Fig. 22), decreasing H_2-pressure below the decomposition pressure (about 3.4 kbar [21]) yields curves with constant CT without deformation: at the given temperatures and pressures the phase transition $\beta \rightarrow \alpha$ occurs. The splitting of the curves in dependence on the measuring direction is caused by loosing H at higher temperatures, if the decomposition pressure increases. The extent of the splitting depends on the relation of measuring time and diffusion rate and on the stage of desorption. In the case of NiFe16at%, the 20.0 kbar curve lifts up (from $M_S = 0$) between 100 and 200°C: at this pressure and this temperature the system passes over from the β-phase to the two phase region ($\alpha\beta$).

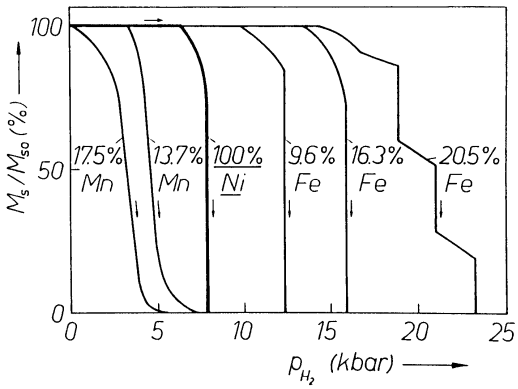

Figure 20. Relative saturation magnetization of Ni, Ni-Fe, and Ni-Mn alloys *versus* hydrogen pressure at about 22°C. Further items see Fig. 19.

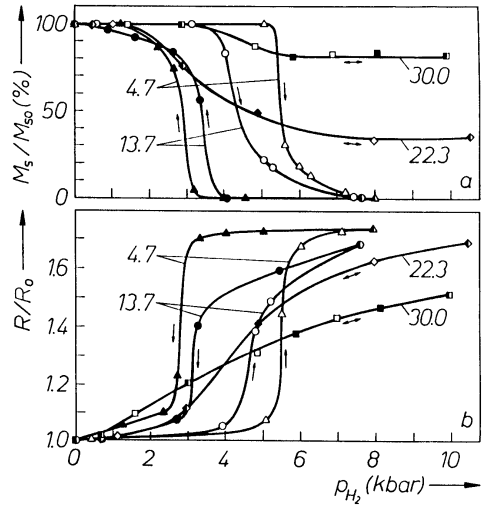

Figure 21. Changes of a) relative saturation magnetization M_S/M_{SO} and b) relative resistance R/R_0 with increasing (open symbols) and decreasing (full symbols) hydrogen pressure for NiMn alloys at about 22°C. M_{SO}, R_0 saturation magnetization and resistance at normal pressure; the parameter is the Mn content in at % (no pressure hysteresis above 20 at % Mn!).

Decreasing H_2-pressure for Ni-Cu (Fig. 23a, above) leads to a shift of *CT*, accompanied by a M_S-*T* shape tendency, similar to that observed in the electrochemically produced system NiCu30at%-H [30] at lower temperatures, indicating a precipitation-like process. In contrast to this, the *CT* remains fixed during pressure reduction in the case of Ni-Mn-H alloy systems, due to a magnetic dominating role of Mn-H interaction [104].

The behaviour of *R*-*T* in all cases studied (as in Fig. 22 and Fig. 23, below) mirrors the magnetic relations: at the Ni-Fe and the Ni-Cu alloy the *disappearance* and the *reappearance* or the 'Ferromagnetic Resistance Anomaly' (*c.f.* [32,33]) or at the disordered NiMn13.7at% alloy, the *conservation* of a *CT* anomaly in spite of relevant changes of average *R*-*T* slope during H absorption and desorption processes, which are also found for the ordered NiMn30at% alloy (which has no *CT* anomaly in the investigated temperature region, Fig. 23, below). The shift of *CT* observed *e.g.* at the

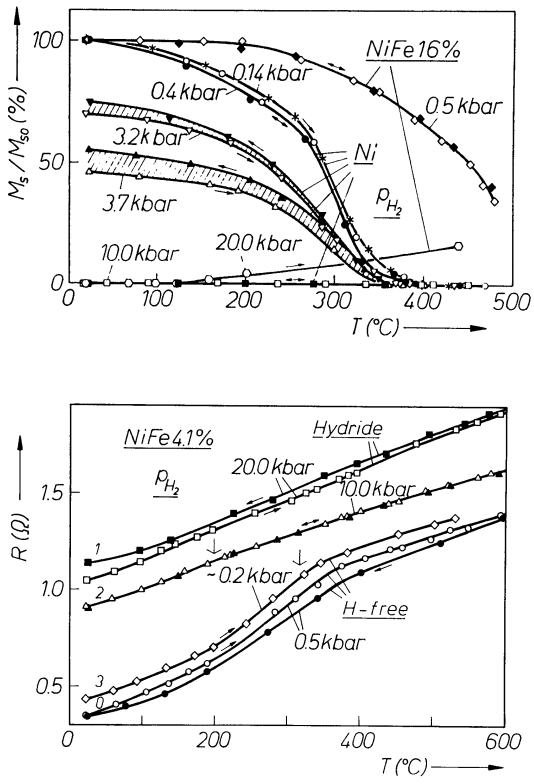

Figure 22. Influence of high pressure gaseous hydrogen on the temperature dependence of saturation magnetization M_S of nickel and a nickel iron alloy (above) and of electrical resistance resp. the 'Ferromagnetic Resistance Anomaly' of a nickel iron alloy (below). M_{SO} saturation magnetization before hydrogen absorption. Sequences of the stationary pressures: above 0.4, 10.0, 3.7, 3.2, 0.14 resp. 0.5, 20.0 kbar; below parameters 0–3. Arrows: approx. position of the Curie temperature (at curve 2 and 3). Average measuring rate: above 50°C min^{-1}; below 16°C min^{-1}.

hydrogenated NiFe4.1at% sample (Fig. 22, below) at about 100°C in the desorption stage of 10.0 kbar H_2 pressure with regard to the position in the phase surface, Fig. 1, corresponds to the findings in [26,59].

The presented examples confirm that measurements of temperature dependence of saturation magnetization M_S and electrical resistance R, including determinations of Curie temperature CT under high pressure hydrogen conditions, deliver sensitive criteria for the respective state of the metal-hydrogen systems and are helpful also for obtaining corresponding phase diagrams.

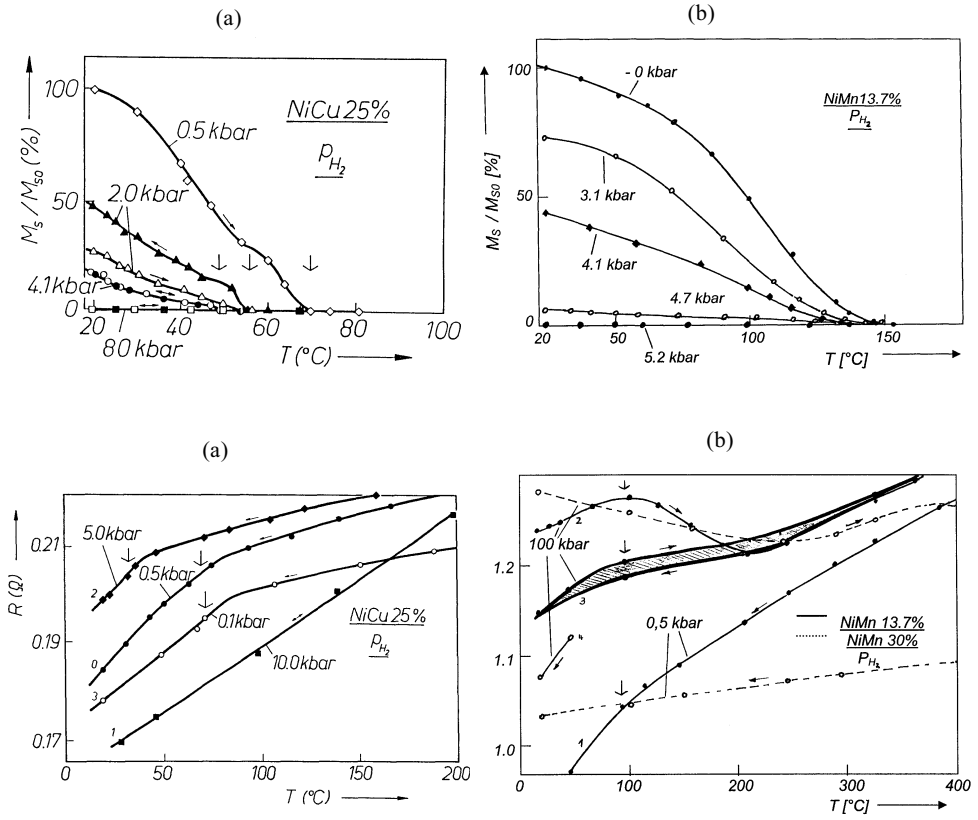

Figure 23. Influence of high pressure gaseous hydrogen on the temperature dependence of saturation magnetization M_S (above) and the electrical resistance resp. the 'Ferromagnetic Resistance Anomaly' (below) of a nickel copper alloy (a) and a disordered NiMn (13.7 at% Mn) alloy (b). Further a corresponding example with respect to the resistance behaviour of an ordered NiMn alloy with 30 at% Mn content (b). M_{SO} saturation magnetization before hydrogen absorption. Sequence of the stationary pressures: above 0.5, 8.0, 4.1, 2.0 resp. 0, 5.2, 4.7, 4.4, 3.1, 0 kbar; below parameters (0–4).

7. Studies about the influence of hydrogen isotopy on nickel-based metal-hydrogen systems

Already in the early sixties – with regard to the basic question of an influence of *hydrogen isotopy* at phase transitions of nickel-based metal-hydrogen systems – Baranowski and co-workers started volumetric measurements of a cathodically effected formation of the *hydride* and *deuteride* phase in Ni, electrochemically deposited on copper supports [40]. The measurements yielded a smaller penetration depth of the deuteride phase. These findings could later be confirmed directly by magnetic 'in situ' measurements on Ni foils [108].

X-ray studies [109] on hydride and deuteride of Ni showed that in analogy to the Pd-H/D systems [110] the lattice spacing in case of nickel deuteride is smaller than in the hydride lattice. Comparing the decomposition kinetics of Ni-hydride and Ni-deuteride and furthermore the formation of Ni-deuteride under high pressure of gaseous deuterium are reported in [111] resp. [112] and summarized in [117].

In addition to the above-mentioned 'in situ'-measurements related to the hydrogen kinetics, one ought to refer to findings – received likewise by the magnetic measuring method – concerning the influence of *hydrogen isotopy* at the formation kinetics of some of the presented systems: In case of cathodic charging of Ni containing 30at% Cu, hydrogen and deuterium can penetrate and form the non-ferromagnetic hydride and deuteride phase *without* the help of any catalytic promotor. That facilitates the interpretation of results. First investigations under these conditions [113] showed a *reversed* kinetic isotope effect, *i.e.* a faster penetration of deuterium into the alloy NiCu30 than of hydrogen.

Such appearance of an inversed hydrogen isotopic effect was hitherto observed in gasvolumetric [114] and electrochemical [115] investigations, only at palladium and its alloys. Oualitatively these results were confirmed by diffusion measurements based on the 'Gorsky effect' [116]. Investigations about diffusion of hydrogen and deuterium in palladium hydride and deuteride under high pressure gaseous hydrogen and deuterium also treated the inversed isotope effect [117].

Within the field of theory there are – besides a semiclassical picture [115][4] – likewise clues for a ratio of diffusion coefficients $D_D/D_A > 1$: Contrary to the classical rate theory [119,120], according to which the light isotope diffuses more quickly than the heavier one independent of temperature, several kinds of quantum corrections of rate theory as *e.g.* the application of quantum statistics [122] and the lattice dynamic theory [123,124] and the evolution of wave packets [125] arose. These quantum corrections reduce the classical isotope effect and become important for small interstitials

[4] It takes into account that during the jump between two atoms of the fcc lattice the interstitial has to overcome a saddle point of energy. There – because of the smaller atomic spacing – the potential flanks are considerably steeper than in the hole of the octahedral sites. In the saddle point the energy levels for the oscillations transverse to the jump direction of the particle are situated higher above the potential minimum than in the starting state. For that reason the light hydrogen needs a higher energy for a jump than deuterium.

(*e.g.* H/D) and low temperature. An extended analysis of non-conventional diffusion mechanism of hydrogen in a metal matrix is given in [126].

As to the question, in which degree the isotope effect observed is really caused by the different velocity of bulk diffusion of the hydrogen isotopes in the NiCu30 alloy, magnetic 'in situ' investigations during cathodic charging under the same conditions as in [113] on foils of different thickness and at different temperatures have been undertaken [127]. In all series of experiments, measurements show that the saturation magnetization decreases more quickly in the case of formation of deuteride than of hydride. Detailed evaluation of results, following known methods [128,129], show that for both isotopes diffusion determines the velocity of absorption. In order to find out the influence of temperature, the Curie temperature of the Ni-Cu alloy, used as well as the electrochemical method, limits the realizable temperature range to a small interval. Nevertheless, a considerable variation of velocity constants with temperature was found. With the assumption of an Arrhenius type behaviour of the absorption, which is probably valid within such a small temperature interval, an apparent activation energy E_a for the absorption process can be calculated. The values of E_a differ slightly for hydrogen and deuterium (H: $E_a = 4.3$ kcal/mol, and D: $E_a = 4.1$ kcal/mol).

The significance of this phenomenon and on the other hand the uncertainity, because of the complexity of electrochemical phase boundary processes, which may already render the absorption rate dependent on isotope, entailed corresponding experiments in high pressure hydrogen/deuterium atmosphere. First experiments realized by 'in situ' resistance measurements on NiCu30-foils under H_2/D_2 gas in the pressure range between 0.8 and 1.2 GPa [130] showed a faster resistance change in the case of the heavier isotope, which also refers to a reversed isotope effect with respect to the hydrogen diffusion in the nickel-copper alloy.

Concerning a possible influence of the surface electron structure on the kinetics of the phase boundary process, magnetic measurements about the time dependence of the interstitial H and D uptake, also in case of Ni-Cr and Ni-Mn cathodic charging[5] [131], showed a decrease of the ratio of the diffusion coefficients D_D/D_H with decreasing temperature. At a sufficiently low temperature, the transition to an inversed isotope effect can be expected.

Generally, the research about the effect of hydrogen isotopy in metal-hydrogen systems should be deepened.

[5] Whereby at NiMnl9.8at% (as before in case of NiCu30at%) the application of a promotor could be renounced, so that no isotope-dependent influence of a promotor may interfere. At NiMnl7.7 resp. 13.7at% the application of a promotor is needed for a sufficient offer of protons able to diffuse at the metal surface: Selendioxid was used to exclude an exchange of light with heavy hydrogen in case of deuterated electrolyte [40], whereby nevertheless a selen deposition during the electrochemical process on the surface of the sample must be taken into account. About investigations concerning the influence of inhibitors in the sense of 'promoters' on the hydride formation at nickel see [132].

In the case of nickel alloys, with a Curie temperature *CT* being, at normal pressure, below the instability temperature of its corresponding hydrides, the whole course of temperature dependence of saturation magnetization (M_S-*T*-curve) can be included for the analysis of 'frozen states' of these metal-hydrogen systems, as shown in the following section.

8. Anomalies of transport properties of hydrides of nickel alloys

This section concerns examples which – as mentioned at the beginning – assign also a special role to phase transitions between hydrogen-free state and hydride with regard to questions of magnetic structures.

So a reincrease of the electrical resistance towards low temperatures (below about 15 K) forming a 'resistance minimum', which was found at nickel hydride already in 1967 at the same time in the laboratories of B. Baranowski and at Munich University [121,122], by means of sensitive magnetic susceptibility measurements, could be identified as resulting from Fe-impurities, which become effective in consequence to the hydrogen-caused cancellation of the ferromagnetism of the Ni-matrix, see Fig. 24 [135]. These results show analogies to those received from diluted Cu(Fe) [136], an alloy with a comparable electronic configuration, and can be interpreted in the sense of a 'Kondo effect', *i.e*. as a spin-flip scattering of conduction electrons on local magnetic moments (between which there is no interaction) [137].

That interpretation has now been tested on the basis of *magnetoresistance* measurements to be described below. Magnetoresistivity is a criterion [136,138] well suited for assessing the share of s-d exchange interaction in the electrical resistivity; its temperature and field dependence is controlled by the response of localized magnetic moments to an external magnetic field.

In supplement to preceding findings [135], the resistance measurements presented in Fig. 25 [139] confirm an interstitial absorption of hydrogen in nickel (cathodically [6] up to an atomic number ratio H/Ni $\geq$ 0.7) in so uniform a cancellation of the nickel matrix ferromagnetism [11], that even small differences in the concentration of the diluted iron solution distinctly manifest themselves in the shape of the minimum – *i.e.* the minimum becomes deeper with increasing concentration. Thus, it varies its temperature position only slightly in agreement with theoretical considerations on comparable diluted alloys [137].

The direct suppression ('freezing out') of the spin-flip scattering by action of a magnetic field upon the 'resistance minimum' could be demonstrated in a work of magnetoresistance [140]: Fig. 26.

A cancelling of the matrix ferromagnetism in *Ni-Cr-alloys* with Cr-contents between 0.5 and 7 at% by interstitial hydrogen leads to a behaviour of the electrical resistance qualitatively similar to that detected at the above-described hydrides of diluted Ni(Fe) alloys showing – although in an even higher temperature region – also an increase of resistance with decreasing temperature after a resistance minimum (Fig. 27 [140]). This *anomalous resistance behaviour* is caused by the hydride state, which

can be explained as the result of an exclusive exchange effect of the conduction electrons with localized magnetic moments of the chromium atoms, which becomes prominent when its original coupling with the surrounding nickel host is cancelled by the interstitial hydrogen. Therefore, a new contribution to the electrical resistance appears for the hydrides, which must be due to the *spin-flip* scattering of conduction electrons at the magnetic moment of the chromium atoms. This contribution increases

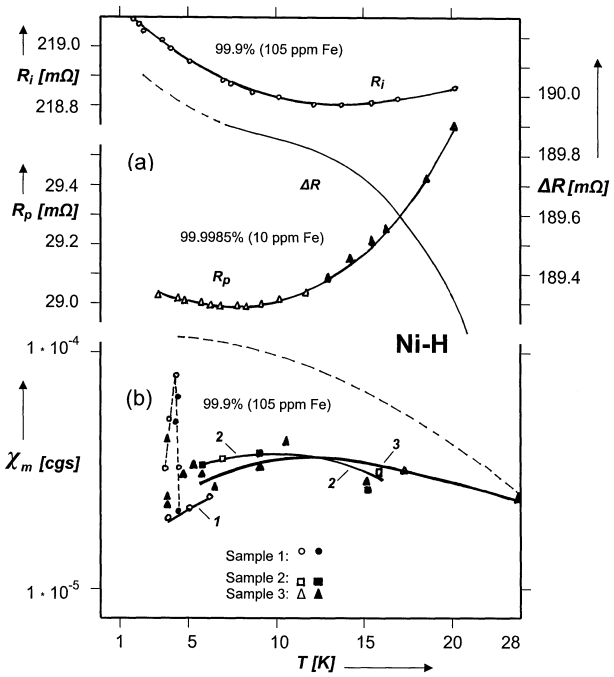

Figure 24. Equivalence of resistance minimum and anomalous temperature dependence of magnetic susceptibility of hydrogenated nickel with 105 ppm Fe [135].
(a) Comparison of low temperature resistance $R_i(T)$ and $R_p(T)$ of an impure nickel hydride sample (with 105 ppm Fe) and a pure one (with only 10 ppm Fe): In spite of deviations of the experimental curve $\Delta R(T) = R_i(T) - R_p(T)$ from the theoretical one [137] below 8 K, a temperature dependence like $\log(T)$ is evident in the range above. The curve $\Delta R(T)$ suggests a Kondo temperature not lower than 15 K.
(b) Susceptibility χ_m of three nickel hydride samples with the same impurity content of 105 ppm Fe as function of increasing (open symbols) and decreasing (solid symbols) temperature as expected shows an increase down to 15 K. Below, a broad maximum refers to the beginning of antiferromagnetic interactions between the impurity atoms and eventually to superparamagnetism or a very weak ferromagnetism of uncharged smallest nickel particles. The susceptibility behaviour below 5 K seems to be connected with the corresponding resistance anomaly. – Dashed line: χ_m course after short-time (16 min) hydrogen desorption showing the disappearance of the susceptiblity maximum by covering the influence of the impurity moments through the occurrence of ferromagnetic coupling, that is already mirrored in ferromagnetic features of corresponding magnetic curves. The results of the resistance and susceptibility measurements turn out to be consistent with respect to the magnetic interaction phenomena and seem to be similar also to such found *e.g.* on diluted alloys of Au with Cr, Mn and Fe [137].

with decreasing temperature. It should be mentioned that *even* for these high chromium concentrations (c) – implying a found Cr-Cr-interaction [139] – the resistance behaviour (with a resistance minimum temperature T_{min} roughly proportional to $c_{1/2}$ [142, Fig. 2] can be understood in analogy to Kondo's theory [137] for diluted alloys.

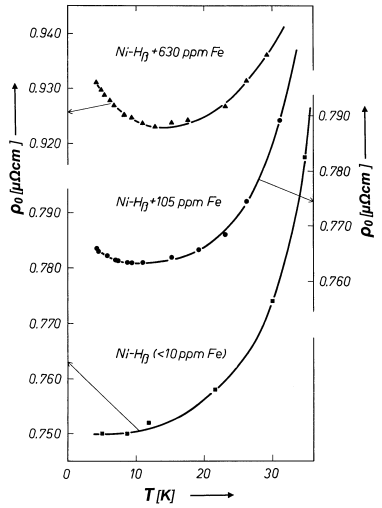

Figure 25. Low temperature shape of electrical resistivity of hydrogenated nickel foils with different iron contents.

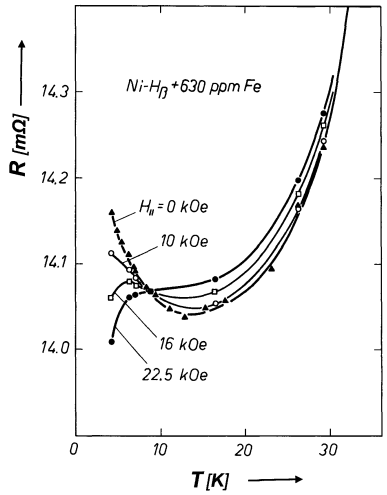

Figure 26. Influence of a longitudinal magnetic field on the 'resistance minimum' produced by cathodic hydride formation at a diluted Ni(Fe)-alloy in the $R(T)$-course. The increase of resistance caused by spin-flip scattering of conduction electrons at local magnetic Fe-moments in the now non-ferromagnetic matrix successively changes into a resistance decrease by freezing out under the action of magnetic fields of increasing strength (parameter), which is manifested in a bend-down of the left flank of the resistance minimum.

In contrast to the *magnetoresistance* of the pure alloys (Fig. 28a)[6], which, in fields above the saturation magnetization (excluding effects due to magnetization processes), show a normal positive magnetoresistance, the longitudinal magnetoresistance of the Ni-Cr hydrides (Fig. 28b) shows a negative course over the whole field range (up to 5 T). This *negative course* of the magnetoresistance of the Ni-Cr hydrides is obviously also the result of a 'freezing out' of the *spin flip* scattering on increasing the magnetic field [142].

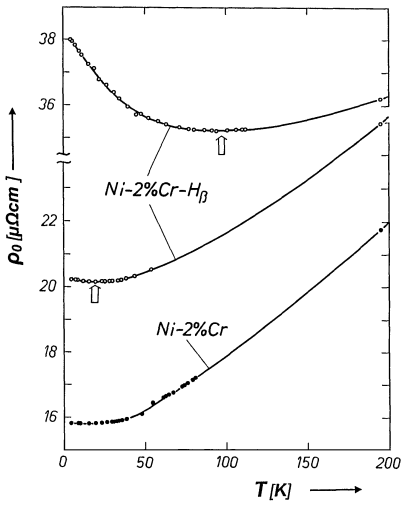

Figure 27. Electrical resistivity of Ni-2at%Cr foils as function of temperature before and after cathodic hydrogen charging. The intermediate curve corresponds to partial desorption.

The separation of the spin portion of the electrical resistance of the Ni-2 at%Cr hydride – on the assumption that Matthiessen's rule is valid – by subtracting the electrical resistance of the pure Ni-2at%Cr alloy and of the Ni-0.5at%Cr hydride[7] leads to the result seen in Fig. 29. From this plot one finds that the characteristic temperature (corresponding the Kondo temperature at diluted alloys) of this system is located between 90 and 100 K, whereby above an irregular spin arrangement in the metal and below the characteristic temperature an exchange between the spins can be supposed [142].

As a further example an alloy of *nickel with 50 at% Cu* may be chosen, where *Ni-clusters* exist, the '*giant moments*' of which are considerably reduced by interstitial hydrogen [144].

The preceding investigations on Ni alloyed with 30 at% Cu have already shown the disappearance of the 'ferromagnetic resistance anomaly' [32], due to the hydro-

[6] S.M. Filipek from the laboratory of B. Baranowski is gratefully acknowledged for the high pressure hydrogenation of the samples.

[7] In the presented case the sample with the lowest Cr-content (of about 0.5 at% Cr) has been drawn upon as reference instead of the pure material, because of the identical preliminary treatment of all samples. Because of the Cr-concentration dependence with the factor 2/0.5, the spin part difference is of small influence.

gen-caused cancellation of the ferromagnetism [33] and its reappearance with a corresponding shift of the Curie temperature during the reduction of the hydrogen content.

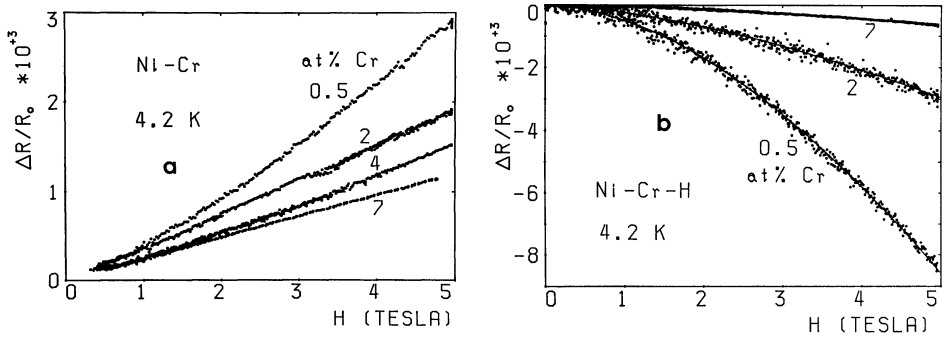

Figure 28. Change of positive (a) to negative (b) longitudinal magnetoresistance R/R_0 at 4.2 K at transfer of ferromagnetic Ni-Cr alloys (here in high pressure gaseous hydrogen) into the non-ferromagnetic hydride phase as an example of the 'freezing-out' of a 'spin flip'-scattering at local magnetic moments by the influence of a magnetic field also in case of non-diluted alloys [142]. R_0 resistance without magnetic field; thickness of sample foils 5–10 μm. The curves drawn in (b) are fits to the measured values describing the magnetoresistance course by functions of the form $\Delta R/R_0 = -a(T,c)H^n$ (where c is the concentration of chromium). The coefficients a and exponents n at 4.2 K were evaluated by double-logarithmic fits to the measured values. The coefficients a and exponents n at 4.2 K were respectively 5.06×10^{-4} and 1.76 for Ni-0.5 at% Cr-H, 2.44×10^{-4} and 1.55 for Ni-2 at% Cr-H and 4.28×10^{-5} and 1.68 for Ni-7 at% Cr-H, which are comparable with experimental and theoretical results for the magnetoresistance of 'spin-glass' alloys such as Cu-Mn and Cu-Fe [143].

In the case of NiCu50at% in the group of Baranowski a low temperature resistance minimum was observed at the neutralization of the matrix ferromagnetism, due to interstitial hydrogen [34]. The pursuit of the investigations on this system [144] shows that the variation of the H-content gives evidence of the influence of interstitial hydrogen on the magnetism of Ni-clusters existing in NiCu50at%[8]. The influence of interstitial hydrogen on the resistance behaviour hereby and during the following stepwise desorption of the hydrogen is shown in Fig. 30a and Fig. 30b and explained in the legends.

According to theoretical considerations concerning Ni clusters in NiCu alloys, a 625 K minimum[8] (here not shown) is produced by a decrease of the spin disorder scattering from cluster moments with increasing temperature, whereas the low temperature behaviour is attributed to a Kondo-like scattering from these cluster moments. In

[8] With growing temperature in $NiCu_x$ from $x = 0.5$ to $x = 0.66$ such giant moment clusters [146] lead to a decrease in R and to a minimum at about 625 K, for x from 0.56 to 0.7, and moreover, to a low temperature minimum [147].

the *hydrogenated* alloy NiCu50-H_n, the monotonous increase of R with growing temperature for $n = 0.16$ and 0.118, as well as the flattening caused by a further diminution of the H-content (desorption), are based on the considerable reduction and then reappearance of cluster magnetism and the spin disorder resistance connected with it. This is a very direct verification of the theoretical work mentioned above [144].

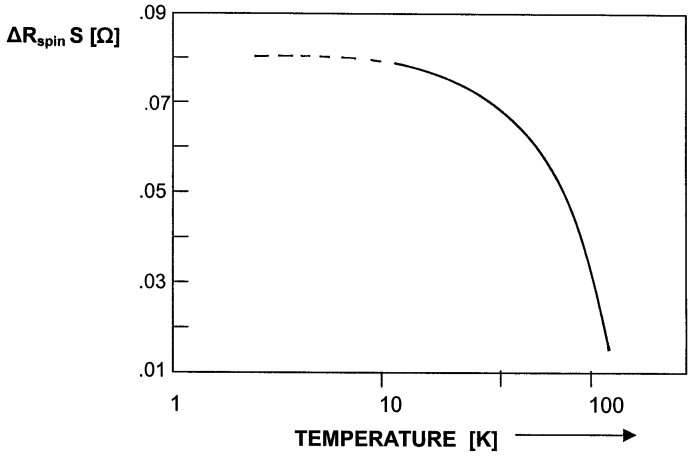

Figure 29. Separated spin contribution ΔR_{spin} to the electrical resistance for the Ni-2at%Cr hydride. The characteristic temperature of this spin can be localized between 90 and 100 K.

In the case of Kondo behaviour of magnetic dilute alloys [137], the dependence of total resistance on temperature is given by

$$R \propto T^5 - c \cdot \log T \tag{4}$$

The second term in equation (4) characterizes the scattering contribution of atomic localized moments (c = concentration of these moments), which grows below the Kondo temperature T_K. In the present investigations, a logarithmic temperature dependence is shown in Fig. 31 [144] for the system NiCu50-H_n with $n = 0.113$, 0.105 and 0.100, and also an accompanying proportionality of the slopes to c according to (4). The following relation, derivable from (4),

$$T_K \propto c^{1/5} \tag{5}$$

is fulfilled only by tendency, because the curves, Fig. 30a, produce a shift in T_K, when they are flattened.

The *Kondo behaviour* in metal-hydrogen systems – as mentioned above – found in diluted Ni(Fe) alloys is based on the *visualization* of atomic Fe-moments in consequence of a complete cancelling of ferromagnetism of the nickel matrix by interstitial hydrogen. In the present investigations, however, Kondo scattering results from

Ni-clusters. Whereas cluster magnetism is dissolved by optimum charging with hydrogen in the limits of our experimental resolution (Fig. 30 a; no minima for $n = 0.16$ and 0.118), Kondo scattering from Ni-clusters appears, when these are already magnetic, but sufficiently small on a magnetic scale (Fig. 30 b; $n = 0.113$, 0.105 and 0.100). By lowering the H-concentration further, the intercluster interaction is finally restored and this is accompanied by the reappearance of Curie points (Fig. 30 b).

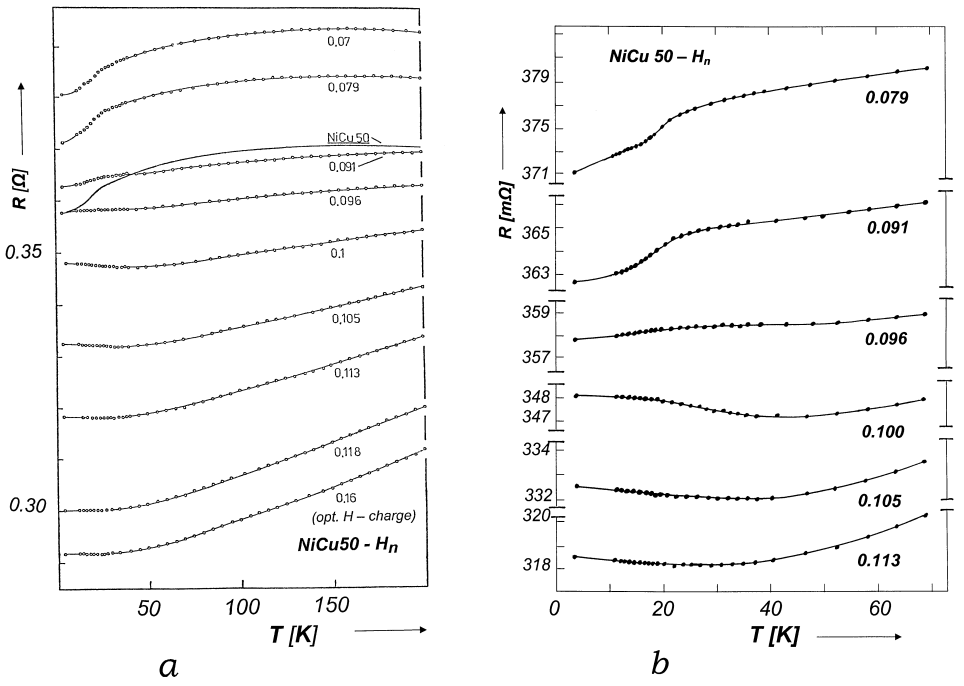

Figure 30. a) Change of the shape of temperature dependence of electrical resistance of a Ni-50 at% Cu-alloy by interstitial hydrogen insertion – over its influence on nickel-clusters – starting from the optimal H-content for NiCu50-H_n (atomic ratio H/Me = $n = 0.16$) to states in which the H-contents, noted as parameter n, are step by step reduced by desorption. NiCu50-$H_{0.16}$ shows no 'ferromagnetic resistance anomaly', thus, also no more Curie point, but compared to NiCu50 above this region, the temperature dependence of resistance is considerably increased. With decreasing H-content the curves get flattened. At $n = 0.113$, 0.105, 0.100 a *Kondo behaviour* by R-minimum gets visible (see also Fig. b), caused by scattering at Ni-clusters with the return of its magnetism. In the course of further reduction of the H-content, the ferromagnetism with Curie temperature reappears.
b) Resistance minima of NiCu50-H_n for a certain H-concentration interval (parameter n) followed by Curie regions, rising again at still lower hydrogen concentrations.

The following refers to the behaviour of *electrical resistance*, *magnetoresistance* and also of *magnetic susceptibility of disordered Ni-Mn alloys* (with manganese contents below 20 at%) also hydrogenated under high pressure conditions [144].

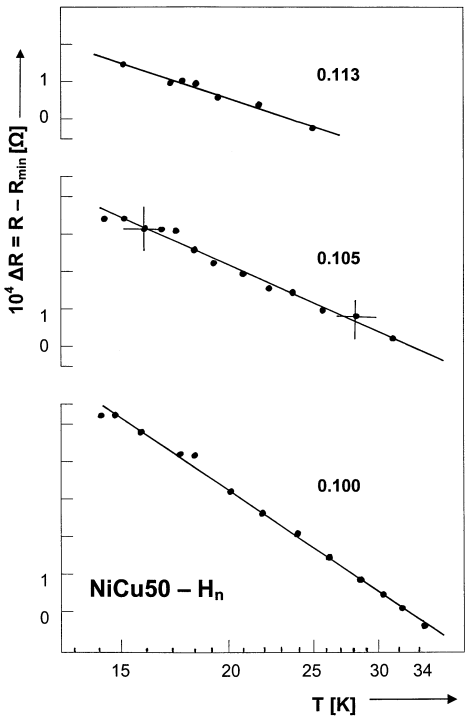

Figure 31. Resistance increase R of three NiCu50-H_n sample states below the minimum temperature T_{min}, with $R_{min} = R(T_{min})$ as a function of temperature in a logarithmic plot: the parameter is n.

Previous investigations [149] of the temperature dependence of the electrical resistance of disordered Ni-Mn alloys in the range of Mn contents between 4.7 and 19.8 at% have shown that *anomalies* of *R(T)* near $T_1 = 20$ K and $T_2 = 50$ K found by Beylin *et al.* [137] and regarded as resulting from an interaction between the magnetic moments of the Mn atoms and the matrix magnetization, withstand the cathodic interstitial hydrogenation in spite of the cancelling of the ferromagnetism [11] connected with a distinct lowering of *R(T)*, see Fig. 32 (above). (In the interest of a better recognizability of the anomalies the results are presented by the temperature dependence of the temperature coefficient of electrical resistance d*R*/d*T*). These observations are probably a sign that a small Ni-area around each impurity has not yet been magnetically neutralized, because the hydrogen could not enter the closest neighbourhood of the impurity [149]. This assumption is supported by observations in [131] on the basis of Mössbauer experiments concerning repulsive interaction between impurities and interstitial hydrogen in case of the Pd-H system.

The application of high pressure hydrogenation of these disordered Ni-Mn alloys in gaseous hydrogen of about 1 GPa leads to a disappearance of the above-mentioned resistance anomaly T_2, Fig. 32 [144]. Obviously the hydrogen activity, which is higher by orders of magnitude in comparison with the cathodic hydrogenation (correspondingly an application of pressures of about 0.6 GPa of gaseous hydrogen [34]),

forces the hydrogen to enter also the closest neighbourhood of the impurity and so to cancel the magnetic moments of the surrounding Ni-area.

Moreover, the remaining shape of the d*R*/d*T(T)* curves (without the anomaly near T_2) of the Ni-Mn alloys hydrogenated under high pressure conditions, also after the desorption of hydrogen, suggests that the hydrogen has resolved the cluster arrangement of the atoms around the 'impurity' atom.

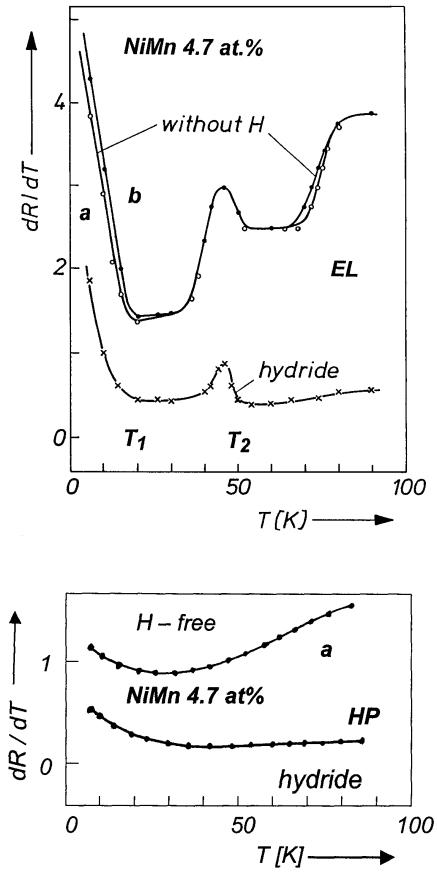

Figure 32. The different influence of cathodic (above) and high pressure hydrogenation (below) on the temperature dependence of the temperature coefficient d*R*/d*T* (0/*K*) of a disordered Ni-Mn alloy. (a after desorption, b before hydrogenation). T_1, T_2: temperatures of the respective clusters producing the anomalies, whereby those at T_2 get destroyed – only under high pressure conditions.

The resistance anomaly near T_1 of this alloy range, however, largely withstands even a high pressure hydrogenation at 1 GPa, accordingly also the *spin glass* character below T_1, by evaluation of resistance measurements remains.

The different withstanding of the anomalies against hydrogenation, such as the preservation of the anomaly near T_1 and on the other hand the desintegration of the anomaly near T_2 support the suggestions that up to T_1 Mn(→)-Mn(→)-clusters and up to T_2 Ni(→)-Mn(→)-clusters (oriented antiparallely to the matrix magnetization) exist in so far as the hydrogen preferentially cancels the magnetic moments of the clustered Ni atoms.

Corresponding to the decrease of the electrical resistance in a *R(T)* graph, the steep rise of the d*R*/d*T* course below about 20 K, as to be seen in Fig. 32, can be interpreted as that occurring in *spin glass* systems [150]. Spin glass behaviour has also been discovered in diluted alloys with transition metals as matrix, as for example in case of PdCr. It is characteristic for such systems, that there is a maximum of the impurity resistivity $\Delta\rho(T) = \rho_{alloy} - \rho_{pure\ metal}$ at low temperatures. This indicates the appearance of magnetic ordering. For comparison, $\Delta R(T) = R(T)_{NiMn(H)} - R(T)_{Ni}$ in the presented case of Ni-Mn (see Fig. 33) shows the same large maximum as observed in the mentioned alloys, too. The analysis of $\Delta R(T)$ with respect to the $T^{3/2}$ law (not shown) also indicates a spin glass interpretation [143][9].

As a result of hydrogenation, it was possible to confirm the tendency – found by analyzing the impurity resistance, Fig. 33 [143] – that interstitial hydrogen has the same consequence on the resistance behaviour of the Ni-Mn alloys as an increase of

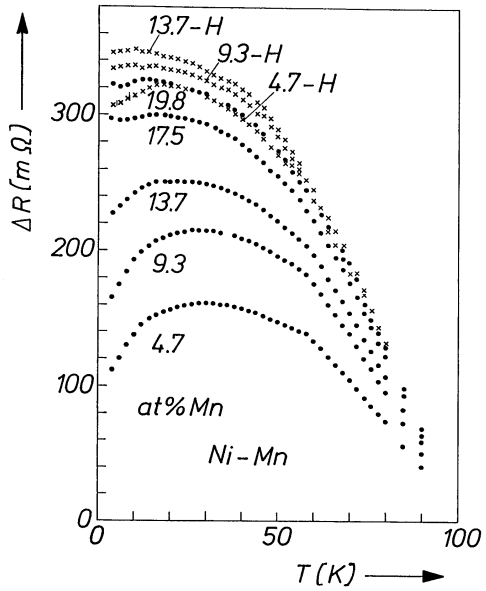

Figure 33. Temperature dependence of $\Delta R(T) = R(T)_{NiMn(H)} - R(T)_{Ni}$ for different Mn concentrations and after hydride formation.

[9] A survey about Spin glasses is given by [143].

the content of (substitutional) Mn atoms in the hydrogen-free alloy also when a magnetic criterion, given by the behaviour of the *longitudinal magnetoresistance* at 4.2 K, Fig. 34 [144], is included.

The negative magnetoresistance (MR) of the H-free Mn alloys (regarded as associated with a decrease of the probability for s-d scattering) increases with increasing manganese content. The hydrogenation magnifies this behaviour for each alloy. The fact, however, that the absorbed H-amount increases with decreasing Mn content, finally leads to a maximal increase of the negative MR for the alloy with the smallest Mn content (4.7 at%). The steep rise of the MR of the H-free samples at low fields,

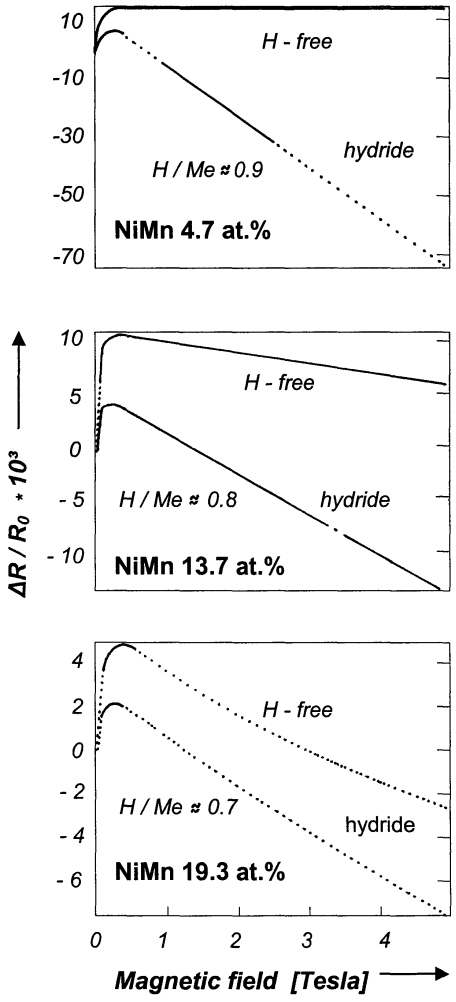

Figure 34. Longitudinal magnetoresistance of disordered Ni-Mn alloys and their hydrides at 4.2 K. The hydrides are formed under hydrogen pressure of 1 GPa with the hydrogen contents H/Me [105] noted in the graphs. R_0 resistance without magnetic field thickness of sample foils 10 μm.

due to ferromagnetic behaviour, gets strongly reduced by the hydrogenation. The remaining part could be related to the manganese.

In view of the apparent spin glass character of this NiMn alloy range, the behaviour of the *reversible magnetic susceptibility* and the corresponding *magnetic hysteresis loop* of high-pressure hydrogenated Ni-Mn13at% alloys, in dependence of the maximal applied magnetic field, is presented in Fig. 35 [144]. The graphs show a drastic irreversible increase of the height of the hysteresis loop by transition from a low magnetic field of about 0.2 Tesla to a high one of nearly 5 Tesla: thus, also after returning again to the low field, the increase shape of the hysteresis remains the same.

This appearance is comparable to observations on $Cu_{0.86}Mn_{0.14}$, interpreted as caused by local cluster effects at this spin glass, also called *'mictomagnet'*.

The examples of this section point out, that interstitial hydrogen cancelling the ferromagnetism of the host matrix of an alloy can reveal correlations, which otherwise remain hidden.

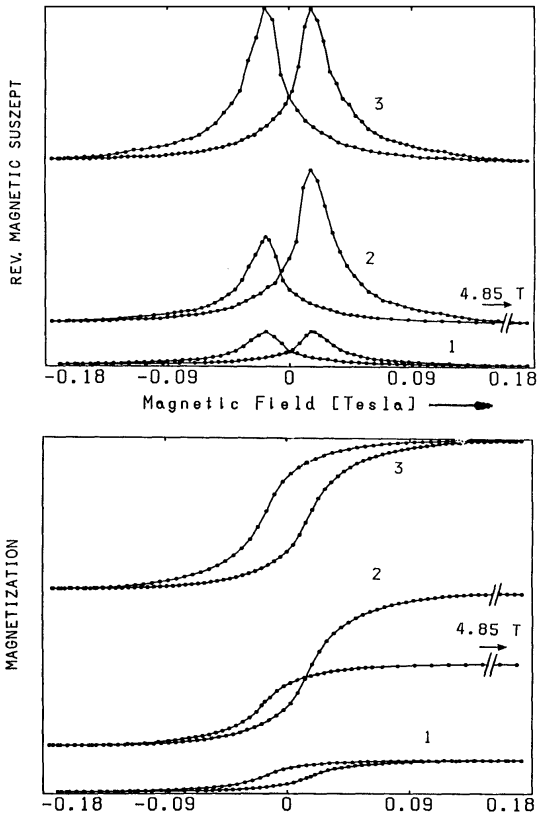

Figure 35. Reversible magnetic susceptibility and magnetization of a Ni-Mn13.7 at% hydride at 4.2 K in dependence of the maximal applied magnetic field. Sequence: 1 low field, 2 high field, 3 low field.

9. Final remarks

The presented investigations generally show, that the role of hydrogen as an alloy partner, or as a sound and sensitive metal-physical partner in connection also with the competitive hydrogenation of the metals by the cathodic method or by application of high pressure, let expect further valuable information.

Therefore, new results in connection with the discovery of electrochemically formed nickel hydride should be taken into consideration, concerning its limited *penetration depth* into the nickel matrix [6] of about 30 micrometers. (The hydrogenation processes reported in this paper are, of course, all placed far below this value). The competition of stresses, caused by the large difference of the lattice parameters (about 7% [16]) at the interface layer of nickel and nickel hydride with a decreasing concentration gradient of hydrogen with its increasing penetration depth may finally lead to a stop of the penetration of the hydride phase. This branch of research was recently continued by B. Baranowski and co-workers by the application of high pressure gaseous hydrogen, in order to extend the penetration depth of the nickel hydride phase into bulk nickel and to find out the thermodynamic conditions for the correlation of the penetration depth of nickel hydride in nickel and the applied pressure of the gaseous hydrogen. These experiments performed at H_2-pressures up to about 12360 ± 80 bars yielded the penetration depth of the nickel hydride into nickel as a linear function of the chemical potential (resp. the logarithm of the fugacity) of the hydrogen, kept in equilibrium with the nickel and, compared to the case of electrochemical hydrogenation, with 59.5 μm finally resulted in a doubling of the penetration depth of the nickel hydride in nickel [152].

Last but not least, basic problems should be kept in mind: So the decrease of the enhanced *paramagnetism* of palladium down to the *diamagnetic* state as hydrogen is inserted [10] raises the question, which final magnetic behaviour the equivalent nickel reaches, when losing its *ferromagnetism* through progressing hydrogenation [11]. The magnetic measurements do not yield a clear distinction between the smallest precipitates of the α-phase and a local fluctuation in the hydrogen occupancy. This motivated magnetic *susceptibility* measurements on optimally hydrogenated nickel of the purest available sort. For minimalizing even small amounts of a ferromagnetic α-phase in the metallurgical system, which would mask the properties of the non-ferromagnetic phase, the application of high pressure hydrogenation was necessary. Thus, in the laboratory of Baranowski, in connection with mass-spectroscopic control, it was possible to receive samples without any detectable ferromagnetism corresponding to less than 10^{-3} of the nickel content in a sample. The measurements of the magnetic susceptibility, performed with the Faraday technique in the field range between 0.9 and 8 kOe, let identify three sources contributing to the magnetic susceptibility. Corresponding conclusions, that there are three different environments in nickel hydride, have also been drawn from experiments using other techniques: *Mössbauer spectroscopy and myon spin rotation*. A minor part, less than 10^{-3} of a sample, consists of small precipitates of the ferromagnetic α-phase (decreasing with

the completion of hydrogenation). Another part is, may be, contributed by the Curie-Weiss temperature dependence of impurities and/or localized magnetic moments on Ni atoms in an environment with some unoccupied hydrogen sites. But the *major part* of the sample comprises the non-ferromagnetic β-phase, showing a temperature-independent paramagnetic susceptibility. From comparison with band structure calculations in [51], it must finally be concluded that nickel hydride can be described as an enhanced Pauli paramagnet.

A closer look at the list of references reveals, how much has been moved in the field of metal-hydrogen systems. This progress was initiated by the discovery of nickel hydride 45 years ago, and it was enhanced by an amazing spectrum of research groups, which were spreading fast now, that the places in the groups VI to VIII of the periodic system of metal-hydrides, that had been empty for such a long time, were filled [1]. In a sense Poland was the "cradle" of new hydrides, and it was in Poland, too, that, due to extended hydrogenation research activities, the surprising and unique discovery was made, that interstitial hydrogen can produce *superconductivity*, in particular in palladium and alloys with nickel [148,150,151].

Finally, it was of equal importance that the first creation of a nickel-based metal-hydrogen system made Baranowski introduce the application of high-pressure hydrogen, which, in its turn, opened a vast field of possibilities and, thus, also prepared the way for creating new hydrides and for investigating them under thermodynamic equilibrium conditions.

Although only a few aspects are described in this paper, it becomes evident that metal-hydrogen research still raises many interesting questions in many different fields.

REFERENCES

1. Mueller W.M., Blackledge J.P. and Libowitz G.G., "Metal Hydrides" Acad. Press, London (1968).
2. Alefeld G. and Völkl J., eds., "Hydrogen in Metals" Vol. I and II, Springer, Berlin (1978).
3. Kirchheim E., Fromm E. and Wicke E., eds., Metal-Hydrogen Systems, Oldenbourg, München, 1988.
4. Fukai Y., "The Metal-Hydrogen System" Springer, Berlin (1993).
5. Wipf H., ed., "Hydrogen in Metals" Vol. III, Springer, Berlin 1997.
6. Baranowski B. and Smialowski M., *Bull. Acad. Polon. Sci. Ser. Sci. Chim. Geol. et Geogr.*, **7**, 663 (1959); *J. Phys. Chem. Solids*, **12**, 206 (1959).
7. Baranowski B., Szklarska-Smialowska Z. and Smialowski M., *Bull. Acad. Polon. Sci. Ser. Sci. Chim., Geol. et Geogr.*, **6**, 179 (1958).
8. Graham T., *Phil. Trans. Roy. Soc.*, **156**, 415 (1866); *Proc. Roy. Soc.*, **16**, 422 (1868).
9. Svensson B., *Ann. Phys.*, **18**, 299 (1933).
10. Lewis F.A., *The Palladium Hydrogen System*, Acad. Press, London, 1967.
11. Bauer H.J. and Schmidbauer E., *Naturwiss.*, **48**, 425 (1961); *Z. Physik*, **164**, 367 (1961).
12. Andrä W., *Phys. Stat. Sol.*, **l**, K125 (1961).
13. Kozlowski L. and Kubiak S., *Bull. Acad. Polon. Sci. Ser. Sci. Math., Astr. et Phys.*, **11**, 235 (1963).
14. Faessler A. and Schmid R., *Phys. Verh.*, **4/5**, 149 (1963); *Z. Phys.* , **l90**, 10 (1966); Nigam A.N., *Curr. Sci.*, **33**, 76 (1964).
15. Janko A., *Naturwiss.*, **47**, 225 (1960); *Bull. Acad. Polon. Sci. Ser. Sci. Chim.*, **8**,131 (1960).
16. Janko A. and Michel P., *Compt. Rend.*, **251**, 1001 (1960).
17. Wollan E.O., Cable I.W. and Koehler W. C., *J. Phys. Chem. Solids*, **24**, 1141 (1963).

18. Baranowski B. and Szklarska-Smialowska Z., *Electrochim. Acta*, **9**, 1497 (1964).
19. Baranowski B., *Bull. Acad. Polon. Sci., Ser. Chim*., **10**, 451 (1962).
20. Baranowski B., *Roczn. Chem.*, **38**, 1019 (1964).
21. Baranowski B. and Bochenska K., *Roczn. Chem.*, **38**, 1419 (1964).
22. Baranowski B. and Bochenska K., *Z. Phys. Chem. N.F.*, **45**, 140 (1965).
23. Baranowski B. and Wisniewski R., *Bull. Acad. Polon. Sci. Ser. Chim*., **14**, 273 (1966).
24. Baranowski B., Bochenska K. and Majchrzak S., *Roczn. Chem.*, **41**, 2071 (1967).
25. Baranowski B. and Bujnowski W., *Roczn. Chem.*, **44**, 2271 (1970).
26. Ponyatovsky E.G., Antonov V.E. and Belash I.T., *Dokl. Akad. Nauk SSSR*, **229**, 391 (1976).
27. Tkacz M. and Baranowski B., *Polish J. Chem*., **66**, 1301 (1992).
28. von Aufschnaiter S. and Bauer H.J., *Z. Angew. Phys*., **17**, 209 (1964).
29. Bauer H.J., Becker M., Pretsch H. and Zwick M., *Phys. Stat. Sol. (a)*, **40**, 445 (1978).
30. Bauer H.J. and Baranowski B., in Proc. Europ. High Presssure Research Group (14th Annual Meeting), W.G.S. Scaife, ed., Typografia Hiberniae, Dublin (1976), p. 3.
31. Bauer H.J. and Baranowski B., *Phys. Stat. Sol. (a)*, **40**, K 35 (1977).
32. Bauer H.J., *Z. Naturforsch*., **22a**, 1468 (1967).
33. Bauer H.J., *Z. Angew. Phys*., **26**, 87 (1969).
34. Skoskiewicz T. and Baranowski B., *Solid St. Commun*., **7**, 647 (1969).
35. Baranowski B. and Majchrzak S., *Roczn. Chem.*, **42**, 1137 (1968).
36. Bauer H.J., Berninger G. and Zimmermann G., *Z. Naturforsch*., **23a**, 2023 (1968).
37. Palczewska W. and Majchrzak S., *Bull. Acad. Polon. Sci. Ser. Sci. Chim*., **17**, G81 (1969).
38. Zimmermann G.J. and Bauer H.J., *Z. Phys*., **229**, 154 (1969).
39. Jonitz D. and Bauer H.J., *Z. Naturforsch*., **33a**, 1599 (1978).
40. Stroka A. and Baranowski B., *Bull. Acad. Polon. Sci., Ser. Chim. Geol. et Geogr*., **10**, 147 (1962).
41. Bauer H.J., Großelfinger I. and Zwick G., *Z. Naturforsch*., **32a**, 343 (1977).
42. Antonov V.B., Belash Z.T., Degtyareva V.F., Ponyatovsky E.G. and Shiryaev V.I., *Dokl. Akad. Nauk SSSR*, **252**, 1384 (1980).
43. Ponyatovsky E.G., Antonov V.E. and Belash I.T., High Pressure Synthesis and Properties of New Hydrides, in: "Problems in Solid State Physics", ed. A.M. Prokhorov and Prokhorov A.S., Mir Publ. Moscow, 1984, p. 109.
44. Belash I.T., Antonov V.E. and Ponyatovsky E.G., *Dokl. Akad. Nauk SSSR*, **235**, 379 (1977).
45. Antonov V.E., Belash I.T., Degtyareva V.F. and Ponyatovsky E.G., *Dokl. Akad. Nauk SSSR*, **239**, 342 (1978).
46. Spitsyn V.I., Antonov V.E., Balakhovsky O.A., Belash I.T., Ponyatovsky E.G., Rashupkin V.I. and Shekhtman V.Sh., *Dokl. Akad. Nauk SSSR*, **260**, 132 (1981).
47. Bauer H.J. and Jonitz D., *Z. Angew. Phys*., **28**, 40 (1969).
48. Ludwig K., Diploma thesis, L.-M.-Univ. München 1980.
49. Bauer H.J. and Thomas U., *Z. Naturforsch*., **21a**, 2106 (1966).
50. Kozlowski L. and Kubiak S., *Bull. Acad. Polon. Sci. Ser. Sci. Math. Astr. Phys.*, **9**, 409 (1961).
51. Bauer H.J. and Ruczka U., *Z. Angew. Phys*., **21**, 18 (1966).
52. Bauer H.J., Pfrenger E. and Stierstadt K., *Z. Naturforsch*., **22a**, 549 (1967).
53. Biedermann E. and Kneller E., *Z. Metallk*., **47**, 760 (1956).
54. Bozorth R.M., Ferromagnetism, D. van Nostrand Co. NY 1951.
55. Jonitz D. and Bauer H.J., *Z. Naturforsch*., **33a**, 1599 (1978).
56. Hutchinson K.L., Lavin P.A. and Moon J.R., *J. Sci. Instrum*., **42**, 6 (1965).
57. Jonitz D. and Bauer H.J., II. Congr. Internat. L'hydrogene dans les Metaux, Paris 8, 1E8 (1977).
57′. Krüger F. and Gehm G., *Ann. Phys*., **16**, a) 174, b) 190, (1933).
57′′. Wollan E.O., *Phys. Rev*., **148**, 517 (1966).
58. Stroka A. and Baranowski B., *Bull. Acad. Polon. Sci., Ser. Chim. Geol. et Geogr*., **10**, 147 (1962).
59. Bauer H.J., Becker M. and Bofilias J., *Naturwiss*., **53**, 17 (1966).
60. Janko A. and Pielaszek J., *Bull. Acad. Polon. Sci., Ser. Sci. Chim. Geol. et Geogr*., **15**, 569 (1967).
61. Pearson W.B., Lattice Spacing and Structures of Metals and Alloys, Pergamon Press 1958.
62. Stroka A., *Bull. Acad. Polon. Sci., Ser. Sci. Chim*., **16**, 65 (1968).
63. Stroka A. and Freilich A., *Roczn. Chem*., **44**, 235 (1970).
64. Bauer H.J., Großelfinger I. and Zwick G., *Z. Naturforsch*., **32a**, 343 (1977).

65. Bomhold G. and Wicke E., *Z. Phys. Chem. NF*, **56**, 133 (1967).
66. Holleck G. and Wicke E., *Z. Phys. Chem. NF*, **56**, 155 (1967).
67. Völkl J., Wollenweber G., Klatt K.-H. and Alefeld G., *Z. Naturforsch*., **26a**, 922 (1971).
68. Majorowski S. and Baranowski B., *J. Phys. Chem. Solids*, **43**, 1119 (1982).
69. Jost W. and Widmann A., *Z. Phys. Chem. Abt*., **B29**, 247 (1935), **B45**, 285 (1940).
70. Wert C. and Zener C., *Phys. Rev*., **76**, 1169 (1949).
71. Vineyard G.H., *J. Phys. Chem. Solids*, **3** , 121 (1957).
72. Le Claire A.D., *Phil. Mag*., **14**, 1271 (1966).
73. Ebisuzaki Y., Kass W.J. and O'Keeffe M.J., *Chem. Phys*., **46**, 1373 (1967); *Phil. Mag*., **15**, 1071 (1967).
74. Pegel B. and Lepski D., *Phys. Stat. Sol*., **23**, 335 (1967).
75. Goltsov V.A. and Smirnov L.I., *II. Congr. Internat. L'hydrogene dans les Metaux, Paris* , **4**, 1C1 (1977).
76. Weiner J.H., *Phys. Rev*., **B14**, 4741 (1967).
77. Kehr J., in "Hydrogen in Metals"', G. Alefeld and J. Völkl, eds., Springer, Berlin (1978) p. 197.
78. Wertheim G.K. and Buchanan D.N.E., *J. Phys. Chem. Solids*, **28**, 225 (1967).
79. Janot Ch. and Kies A., in Proccedings of the International Conference on Hydrogen in Metals (Editions Science and Industrie, Paris 1972), p. 204.
80. Mizutani T., Shinjo T. and Takada T., *J. Phys. Soc. Japan*, **43**, 794 (1976).
81. Amer M.A., Wagner F.E. and Bauer H.J., *Hyp. Int.*, **41**, 539 (1988).
82. Karger M., Pröbst F, Schüttler B. and Wagner F.E. , in Veziroglu (ed.), Metal-Hydrogen Systems (Pergamon Press, Oxford) 187 (1982).
83. Pröbst F., Wagner F.E. and Karger M., *J. Less-Comm. Met*., **88**, 201 (1982).
84. Pröbst F. and Wagner F.E., *J. Phys. F: Met. Phys*., **17**, 2459 (1987).
85. Tröger J., Karger M., Butz T. and Wagner F.E., *Hyp. Int*., **15/16**, 795 (1983).
86. Amer M., Baier M., Bauer H.J. and Wagner F.E., *Z. Phys. Chem. NF*, **164**, 773 (1989).
87. Martin W.E. and Bauer H.J., in Int.Conf. "H4, Hydrogen and Materials", Beijing 1988, Azou P.Y. and Chen N.P., eds., ISMCM, Saint-Quen, France (1989) p. 110.
88. Zhang B., Bauer H.J., Baier M., Wagner F.E., Antonov V.E. and Antonova T.E., *J. Less-Comm. Met.*, **172–174**, 341 (1991).
89. Zhang B., Dugandzic I., Bauer H.J., Baier M., Wagner F.E., Antonov V.E., Antonova T.E. and Filipek S.M., *Hyp. Int*., **69**, 471 (1991).
90. Schneider G., Baier M., Wagner F.E., Dugandzic I., Bauer H.J., Antonov V.E., Antonova T.E. and Filipek S.M., *Z. Phys. Chem*., **179**, 301 (1993).
91. Shenoy G.K., Wagner F.E. and Kalvius G.M., in Shenoy G.K. and Wagner F.E. (eds.) Mössbauer Isomer Shifts, North Holland, Amsterdam (1978) p. 49.
92. Bauer H.J. and Schenk H.J., *II. Congr. Internat. L'hydrogene dans les Metaux, Paris*, **8**, E2 (1977).
93. Dünnwald H. and Wagner C., *Z. Phys. Chem*., **B24**, 53 (1934).
94. Baranowski B., *Bull. Acad. Polon. Sci. Ser. Sci. Chim*., **7**, 887 and 907 (1959).
95. Dugandzic I., Filipek S.M. and Bauer H.J., High Pressure Research, **4**, 493 (1990).
96. Rani-Srivastava R., Dugandzic I., Müller R., Taliantzis E. and Bauer H.J., Scientific and Technical Seminar "Diffusive-Cooperative Phenomena in the Systems Metal-Hydrogen Isotopes",'Metal-Hydrogen 92'; Donetsk, Ukraine, 15–19 Sept. 1992, Part 1, p. 12; Müller R., Diploma thesis, L.-M.-Univ. München 1986, Taliantzis E., Diploma thesis, L.-M.-Univ. München 1984.
97. Jarmolowicz H. and Smialowski M., *J. Catal.*, **1**, 165 (1962).
98. Gerlach W.,*Z. Metallk.*, **29**, 102, and 124 (1937); *Z. Metallk.*, **30**, 77 (1938); *Z. Metallk.*, **40**, 281 (1949).
99. Bozorth R.M., Ferromagnetism, The Bell Laboratories Series (1951).
100. Hoselitz K., Ferromagnetic Properties of Metals and Alloys, Clarendon Press, Oxford (1952).
101. Berkowitz A.E. and Kneller E., Magnetism and Metallurgy, Acad. Press, NY (1969).
102. Martin W.E., Bauer H.J., Filipek S.M. and Baranowski B., *J. Less-Comm. Met*., **103**, 259 (1984).
103. Martin W.E. and Bauer H.J., *Z. Phys. Chem. NF*, **147**, 179 (1986).
104. Martin W.E., Bauer H.J., Filipek S.M. and Baranowski B., *J. Magn. Magn. Mat.*, **54–57**, 1505 (1986).
104′. Antonov V.E., Belash I.T., Degtyareva V.F., Ponyatovsky E.G. and Thiessen V.G., *Phys. Met. Metall.*, **53**, 47 (1982).
105. Martin W.E., Bauer H.J. and Filipek S.M., in 'Material Properties/ Materials Design' B. Wu, ed., Elsevier Science Publ. B.V., 747 (1991).

106. Martin W.E. and Wieser J.,*J. Phys. E: Sci. Instrum* ., **18**, 342 (1985); *J. Phys. E: Sci. Instrum*., **15**, 639 (1982).
107. Baranowski B. and Tkacz M., *Z. Phys. Chem. NF*, **135**, 27 (1983).
108. Filipek S.M., Bauer H.J. and Baranowski B., in*Mat. Res. Soc. Symp. Proc*., **22**, 'High Pressure Science and Technology', Part 1, C. Homan, R.K. MacCrone and E. Whalley, eds., North-Holland, NY (1984), 115.
109. Filipek S.M., Bauer H.J., Majchrzak S.M. and Yamamoto H., *Z. Phys. Chem. NF*, **163**, 485 (1989).
110. Filipek S.M., Szafranski A.W., Warsza M. and Majchrzak S., *J. Less-Comm. Met.*, **158**, 177 (1990).
111. Bauer H.J. and Baranowski B., in 'High Pressure Science and Technology', **1**, K.D. Timmerhaus and H.S. Barber, eds., Plenum Press, NY (1979), 248. –'II. Congr. Internat. L'hydrogene dans les Metaux', Paris **8**, 1E1 (1977).
112. Baranowski B. and Filipek S.M., *Roczn. Chem.*, **47**, 2165 (1973).
113. Bauer H.J., *J. Phys. E: Sci. Instrum*., **10**, 332 (1977).
114. Bauer H.J., *J. Magn. Magn. Mat*., **15–18**, 1267 (1980).
115. Schenk H.J., Bauer H.J. and Baranowski B., *Phys. Stat. Sol. (a)*, **52**, 195 (1976).
116. Schenk H.J. and Bauer H.J., *Z. Phys. Chem. NF*, **115**, 213 (1979).
117. Schenk H.J., Bauer H.J. and Baranowski R., in "High Pressure Science and Technology", B. Vodar and Ph. Marteaux, eds., Pergamon Press, Oxford and NY (1980), 444.
118. Krukowski M. and Baranowski B., *Roczn. Chem*., **49**, 1183 (1975); *J. Less-Comm. Met.*, **49**, 385 (1976).
119. Bauer H.J., Schenk H.J. and Baranowski B., *Trans. Jpn. Inst. et., Suppl*., **21**, 377 (1980).
120. Bauer H.J., in "Metal Hydrides", G. Bambakidis, ed., NATO Advanced Study Institutes Series, Ser. B 76, Plenum Press, NY (1981), 313.
121. Baranowski B. and Szymaszek J., *Phys. Stat. Sol*., **20**, K37 (1967).
122. Bauer H.J. and Bauer K.H.W., *Z. Naturforsch*., **22a**, 575 (1967).
123. Bauer H.J., Kohler K.A., Dietrich I. and Kadereit H.G., *Phys. Letters*, **31A**, 57 (1970); *Z. Angew. Phys*., **30**, 32 (1970).
124. a) Daybell M.D. and Sueyert W.A., *Phys. Rev*., **167**, 536 (1968), b) *Phys. Rev. Lett*., **20**, 195 (1968).
125. Kondo J., *Prog. Theor. Phys* ., **32**, 37 (1964).
126. Van Den Berg G.J., Proc. 9th Internat. Conf. Low Temp. Phys., Part B, Plenum Press, NY 1965 (p. 933).
127. Beal-Monod M.-T. and Weiner R.A., *Phys. Rev*., **170**, 552 (1968).
128. Kohler K.A. and Bauer H.J., *Phys. Stat. Sol. (a)*, **14**, K27 (1972).
129. Bauer H.J. and Kohler K.A., *Phys. Lett. A*, **41**, 291 (1972).
130. Schwarz D.K. and Bauer H.J., *J. Less-Comm. Met.*, **103**, 375 (1984).
131. Daniel H.-U. and Bauer H.J., *J. Magn. Magn. Mat.*, **6**, 302 (1977).
132. Hicks T.J., Rainford B., Kouvel J.S., Low G.G. and Comly J.B., *Phys. Rev. Lett*., **22**, 531 (1969).
133. Kouvel J.S. and Comly J.B., *Phys. Rev. Lett*., **24**, 598 (1970).
134. Houghton R.W., Sarachik M.P. and Kouvel J.S., *Phys. Rev. Lett*., **25**, 238 (1970); *Solid State Commun*, **8**, 943 (1970).
135. Levin K. and Mills D.L., *Phys. Rev*., **B9**, 2354 (1974).
136. Csuzda I. and Bauer H.J., in P. Jena and C.B. Satterthwaite, eds., Electronic Structure and Properties of Hydrogen in Metals, Plenum, NY (1983), 653.
137. Beylin V.M., Rogelberg I.L. and Cherenkov V.A., *Sov. Low Temp. Phys*., **4**, 11 (1978); Beylin V.M., Zeynalov T.I., Rogelberg I.L. and Cherenkov V.A., *Phys. Met. Metall. Vol.,* **46**, 5, 163 (1979).
138. Wagner F.E., Karger M., Probst F. and Schuttler B., paper FR-27, 'Internat. Symposium on the Electronic Structure and Properties of Hydrogen in Metals', Richmond, Virginia, March 4–6, 1982.
139. Roshko R.M. and Wiliams G., *Phys. Rev. B*, **15**, 1503 (1977).
140. Csuzda I., Diploma thesis, L.-M.-Univ. München 1980.
141. Fischer K.H. and Hertz J.A.,'Spin Glasses', Cambridge University Press 1991.
142. Schwarz D.K., Dugandzic I., Filipek S.M. and Bauer H.J., Proc. XV AIRAPT Conference, Warsaw 1995, W. Trzeciakowski, ed., World Scient. Publ. Co, Singapore 1996, p. 736.
143. Mott N.H., *Proc. Roy. Soc*., **A 153**, 699 (1936).
144. Schulze U., Felton G. and Schwink Ch., *J. Magn. Magn. Mat*., **15–18**, 205 (1980).
145. Stroka A. and Baranowski B., Proc. XV AIRAPT Conference, Warsaw 1995, W. Trzeciakowski, ed., World Scient. Publ. Co., Singapore 1996, p. 536.

146. Hanson M. and Bauer H.J., *J. Phys. (Paris), Colloq. C8*, **49**, 125 (1988); *J. Alloys and Comp*., **179**, 339 (1992).
147. Spunar B., Wallace W.E. and Strange P., *J. Less-Comm. Met*., **123**, 37 (1986).
148. Skoskiewicz T., *Phys. Stat. Sol. (a)*, **11**, K123 (1972).
149. Skoskiewicz T. and Baranowski B., *Phys. Stat. Sol*., **30**, K33 (1968).
150. Skoskiewicz T., Szafranski A.W., Bujnowski W. and Baranowski B., *J. Phys. C: Solid State Phys*., **7**, 2670 (1974).
151. Baranowski B. and Skoskiewicz T., High Hydrogen Pressures in Superconductivity in High-Pressure and Low-Temperature Physics, eds. C.U. Chu and J.A. Wollam (Plenum Press, NY 1978) p. 43.
152. Stroka A. and Baranowski B., *Polish J. Chem*., **76**, 1019 (2002).